Lawrence Berkeley National Laboratory
Recent Work

Title
THE PHYSICS OF JETS

Permalink
https://escholarship.org/uc/item/20w7r2tv

Author
Hofmann, W.

Publication Date
1987-09-01

eScholarship.org Powered by the California Digital Library
University of California

LBL-23922

Lawrence Berkeley Laboratory
UNIVERSITY OF CALIFORNIA

Physics Division

RECEIVED
LAWRENCE
BERKELEY LABORATORY
NOV 10 1987
LIBRARY AND
DOCUMENTS SECTION

Invited talk presented at the International Symposium on Lepton and Photon Interactions at High Energies, Hamburg, FRG, July 27–August 3, 1987

The Physics of Jets

W. Hofmann

September 1987

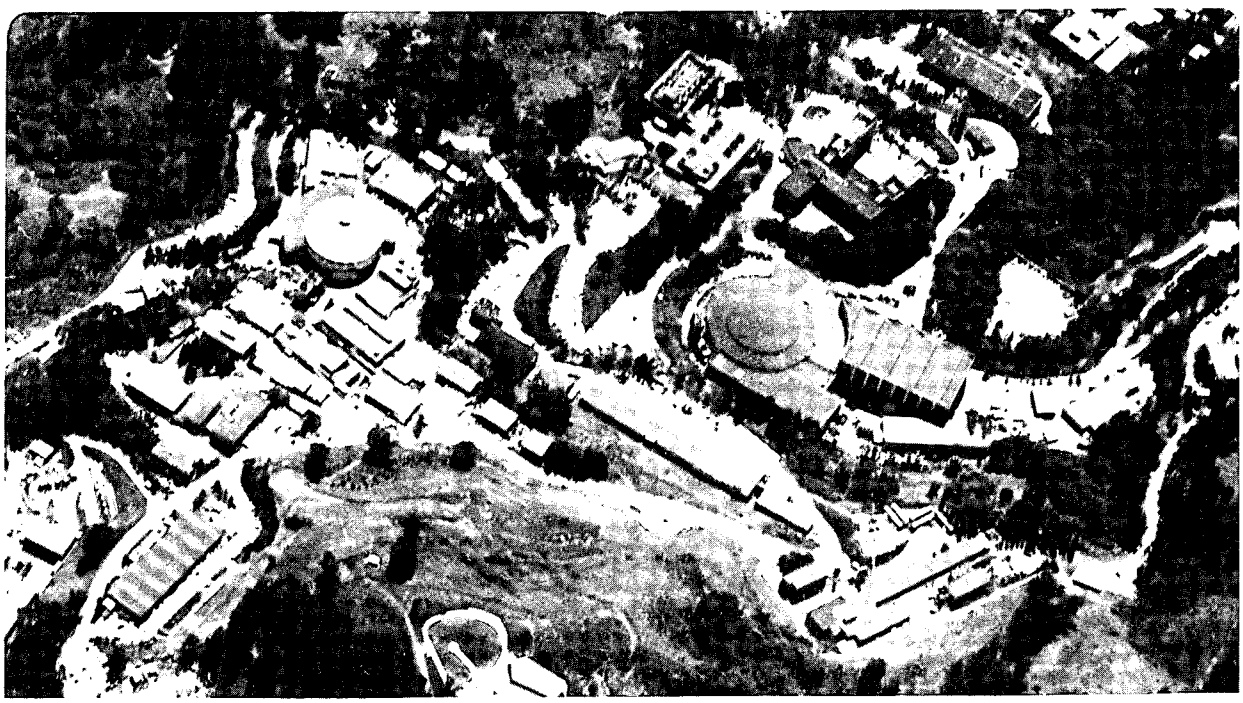

Prepared for the U.S. Department of Energy under Contract DE-AC03-76SF00098

LBL-23922

DISCLAIMER

This document was prepared as an account of work sponsored by the United States Government. While this document is believed to contain correct information, neither the United States Government nor any agency thereof, nor the Regents of the University of California, nor any of their employees, makes any warranty, express or implied, or assumes any legal responsibility for the accuracy, completeness, or usefulness of any information, apparatus, product, or process disclosed, or represents that its use would not infringe privately owned rights. Reference herein to any specific commercial product, process, or service by its trade name, trademark, manufacturer, or otherwise, does not necessarily constitute or imply its endorsement, recommendation, or favoring by the United States Government or any agency thereof, or the Regents of the University of California. The views and opinions of authors expressed herein do not necessarily state or reflect those of the United States Government or any agency thereof or the Regents of the University of California.

LBL-23922

The Physics of Jets

W. Hofmann

Lawrence Berkeley Laboratory
University of California
Berkeley, CA 94720

September 1987

Invited Talk at the
International Symposium on Lepton and Photon Interactions at High Energies
Hamburg, July 27 - August 3, 1987

ABSTRACT

Recent data on the fragmentation of quarks and gluons is discussed in the context of phenomenological models of parton fragmentation. Emphasis is placed on the experimental evidence for parton showers as compared to a fixed order QCD treatment, on new data on inclusive hadron production and on detailed studies of baryon production in jets.

1. INTRODUCTION

The creation of jets of hadrons in e^+e^- annihilation events (such as the one shown in Fig. 1) begins with the production of a pair of primary quarks by the virtual photon produced in the annihilation. Because of the large momentum transfer involved, these quarks are usually highly virtual; they cascade down to the mass shell by successive emission of gluons, which in turn may be off-shell and branch into two new gluons or another pair of quarks, and so on, until all partons of the cascade are close to their mass shell. This process can be described in perturbative QCD, either in terms of a fixed-order calculation or in terms of a parton "shower"[1]. Below a certain virtuality, the relevant coupling constant, α_S, becomes large and perturbative expansions are no longer valid. A nonperturbative mechanism sets in and turns the quarks and gluons of the parton shower into primary hadrons. Finally, these hadrons decay and give rise to the observed stable particles. The boundaries between the perturbative and the nonperturbative phase, and to some extent the distinction between the final stages of confinement and the early stages of particle decay chains, are somewhat arbitrary and reflect the limitations of our understanding rather than true differences in the underlying physics. The main goals behind the "physics of jets" are thus to test techniques developed in perturbative QCD, and to derive a deeper knowledge as well as phenomenological models of the nonperturbative regime. As an occasional fringe benefit, we may learn something new about particles and their decays.

In this review of recent results, I will address four main topics:

- Properties and phenomenological relevance of parton showers as compared to fixed-order calculations in perturbative QCD.
- New results on inclusive hadron production as a test of fragmentation models.
- Ways to probe the dynamics of the hadronization process using baryons in quark and gluon jets.
- New ideas on the phenomenology of the fragmentation process.

I will concentrate on jets in e^+e^- annihilation and, to some extent, in deep inelastic scattering, since those reactions provide the cleanest environment for the study of high-energy quark jets.

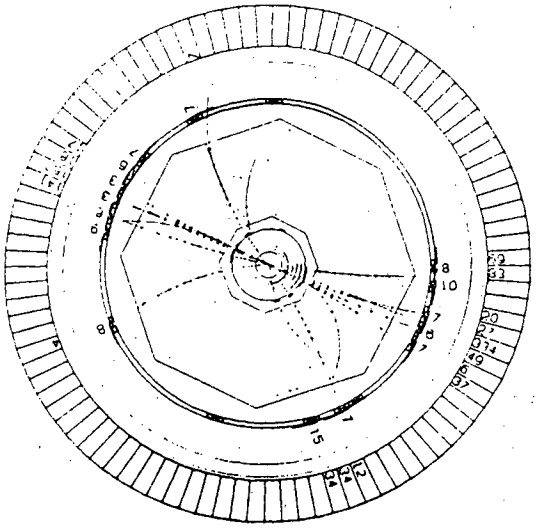

FIGURE 1

Typical jet event observed in e^+e^- annihilation at $\sqrt{s}$ = 52 GeV in the TOPAZ detector at TRISTAN, viewed along the e^+e^- collision axis.

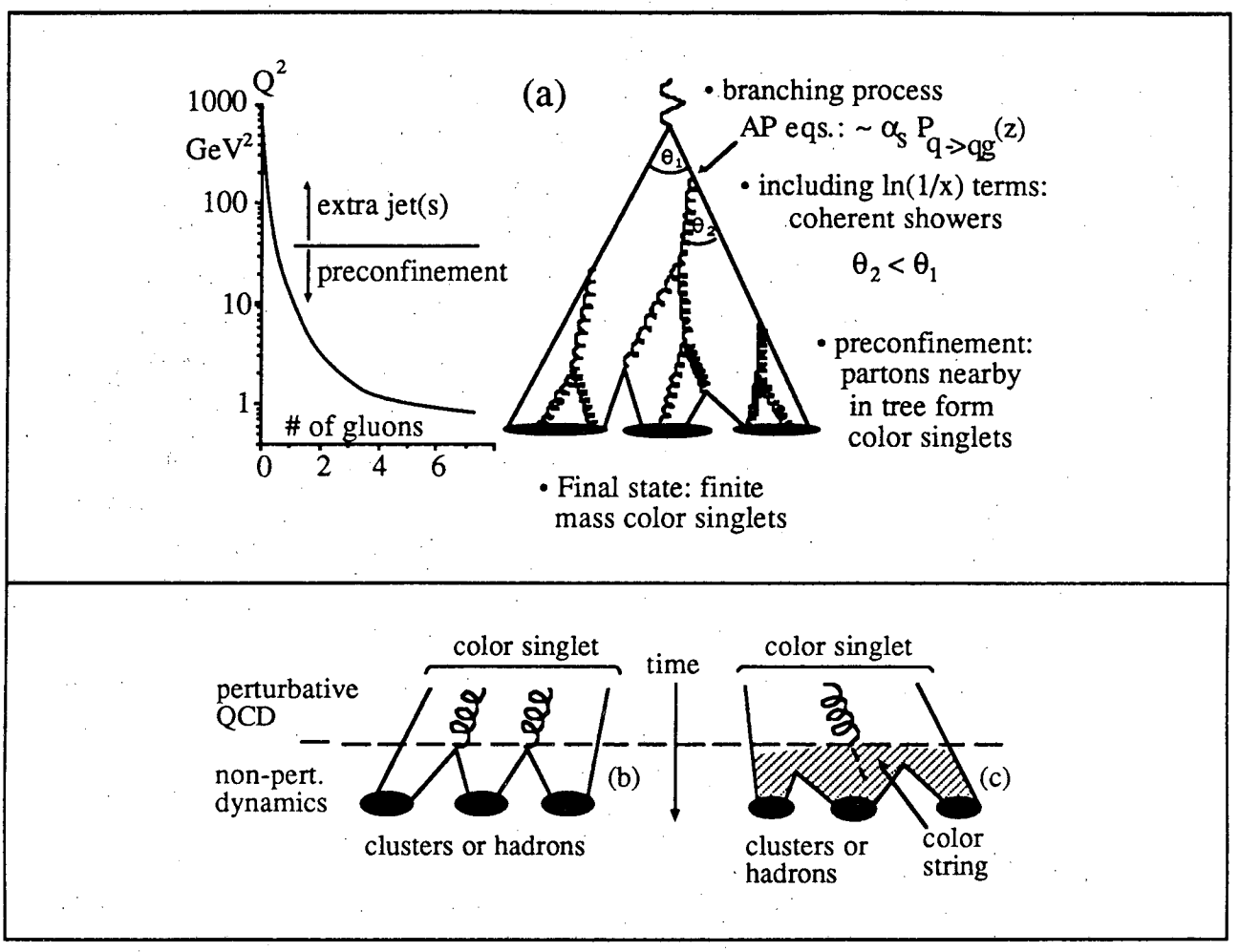

FIGURE 2

(a) Evolution of a parton shower via successive branching, ending with the formation of color singlets. The scale on the left indicates parton virtualities; also shown is the average number of gluons in the shower as a function of the virtuality cutoff Q^2. (b) Hadronization of color singlet systems in QCD cluster models. (c) Hadronization of color singlet systems in string models

2. PHENOMENOLOGY OF PARTON FRAGMENTATION

Let me first review the phenomenology in a little more detail. Concerning the perturbative evolution, I will concentrate on the concept of parton showers, given that fixed-order calculations i) are covered in other talks at this conference and ii) are of limited usefulness as the available cms energies increase beyond the PEP/PETRA range. The main features of parton showers are summarized in Fig. 2(a). The evolution of partons towards their mass shell is described as a branching process[1] governed by the Altarelli-Parisi equations[2], which account for collinear singularities in the leading-log approximation. Over the last few years, one has also learned[3] to deal with leading infrared singularities; those developments have resulted in the notion of a "coherent" or angular-ordered shower, as compared to "conventional" parton showers. In coherent showers the emission angles decrease monotonically for successive branchings. This additional constraint reduces the phase space for parton emission and effectively accounts for interference effects. This is particularly easy to visualize for the first $q \rightarrow qg$ branching: obviously, by the time the first gluon is emitted, the separation between quark and antiquark must be at least of the order of the gluon wavelength, otherwise quark and antiquark will act as a color singlet and not emit gluons. A short semi-classical calculation shows that (in the infinite-momentum frame) this condition is equivalent to the ordering of angles, $\theta_1 > \theta_2$. Near the end of the shower, angular ordering reduces the phase space for gluon emission and hence the number of soft gluons drastically. Parton showers exhibit another interesting property: preconfinement[4], a precursor to color confinement within perturbative QCD. Partons nearby in the tree structure can be shown to form color singlets consisting of a quark, an antiquark, and a number of gluons (Fig. 2(a)). The average mass of these singlets approaches a finite limit as the cms energy of the entire cascade increases; this means that at higher energies one will have more of these singlets, but their properties remain the same. Unfortunately, for typical virtuality cutoffs around $Q^2 \approx 1$ GeV^2 (at significantly lower values, perturbation theory will break down), the mass of these color singlets is fairly large and the singlets cannot be identified with hadrons. In fact, typical events at PEP or PETRA energies contain one or at most two such color singlet systems. The reason is that the number of singlets is given by $n_{q\overline{q}} + 1$, where $n_{q\overline{q}}$ is the number of new $q\overline{q}$ pairs produced in the shower. Because of the small quark-gluon coupling (compared to the strength of the triple-gluon vertex), quark pair production is a rather infrequent process in a shower, which evolves mainly via $g \rightarrow gg$. The average number of gluons in a parton shower in the PEP/PETRA energy range is shown in Fig. 2(a), as a function of the virtuality cutoff Q^2 [5]. Above a cutoff around 30 GeV^2, the gluon multiplicity is small; those gluons will show up as extra jets in the events. At later stages, the number of gluons increases up to 5 to 10 per event; these gluons are no longer visible as extra jets, but they still influence the overall kinematic structure of the events.

Whereas the basic ideas of a parton shower seem straightforward - a quark of virtuality Q^2 emits a gluon according to a splitting kernel $P_{q\to qg}(z)$, governed by the strong coupling α_s - the actual implementation as a stochastic process reveals an infinity of ambiguities[6,7], the resolution of which lie beyond the approximations presently used. For example, the energy-sharing variable z is well defined only in the limit of infinite energies and collinear kinematics; for finite emission angles, the interpretation of z as a light cone fraction, an energy fraction or a momentum fraction yield significantly different results. Most definitions of z are not Lorentz invariant, so that one also needs to specify the frame in which z is evaluated. The same problem occurs with the ordering of angles - after all, the order may be frame-dependent! The coupling constant α_s needs to be evaluated at some scale; unfortunately, there are several large mass scales in the problem, such as the virtuality of the parent parton or the transverse momentum of the decay products (within the framework of coherent showers, one can argue in favor of the latter choice[8]). The kinematics of the process is a nightmare; after all, the virtualities of the daughter partons are only known after those partons decay (the decay can be understood as a first "measurement" of their mass); however, the phase space for the decay of the parent and hence its decay rate depend on the masses of the daughters. For this reason, early Monte Carlo shower generators[9] reconstructed the entire shower tree backwards, starting from the masses of the final partons. More recent implementations[10],[11] redefine the interpretation of z in order to avoid inconsistencies. Finally, the leading-log approximation fails drastically for the first large-angle gluon emission, resulting in 3-jet event rates inconsistent with fixed-order QCD. These problems have been discussed by various authors[6,9,11] and were addressed systematically in a paper submitted to this conference[7]. Many of the differences between the early conventional and the coherent shower algorithms are really due to different implementations of those "technical details" and not due to the angular ordering. For example, the average gluon multiplicity in a 100 GeV shower may vary by factors 3-4 depending on how the splitting variable and the mass scales are defined; on the other hand, switching coherence on and off (and leaving everything else the same) changes the average number of gluons by less than 50% [7]. A consensus seems to emerge that while ultimately data may help to pin down some of the choices, at any fixed energy different algorithms can be brought into close agreement (concerning the number of partons in the shower and their spectra) by adjusting the virtuality cutoff[7,11,12], which should be considered as an *ad hoc* parameter. Distinguishing between details of shower models experimentally will require a tremendous lever arm in cms energy (from some 10 GeV up to some TeV, say).

In any case, in order to model parton fragmentation one has to deal somehow with the color singlet systems resulting from the shower evolution. The fundamental idea is always the same: the starting point is a system made of a quark, an antiquark and the gluon field "in between". Somehow, the gluons will create new quark-antiquark pairs and, following the planar color flow, each

quark will have an antiquark neighbor nearby in phase space with which it forms a color singlet state[4]. If the number of new pairs is sufficiently large, the mass of those singlets will be in the GeV range and they can be identified either with known hadrons, or with clusters (excited meson states, somewhat along the lines of Hagedorn's bootstrap model), or with a mixture of both. The two flavors of available models differ mainly in their description of the gluon field: "QCD cluster models"[13] simply split the gluons remaining after the perturbative evolution into quark-antiquark pairs (or sometimes into diquark-antidiquark pairs) and thus extend the preconfinement mechanism one step further (Fig. 2(b)). Members of this category are the Webber model and the (meanwhile more or less extinct) Fox-Wolfram[14], Field-Wolfram[15], and CALTECH I[16] models. The decay of the clusters is often described as a two-body phase space decay into hadrons or lower-mass clusters, resulting in a refreshingly small number of free parameters (the Webber model has about 5 adjustable parameters, compared to about 15 in the Lund model to be discussed later [17]).

On the other hand, "string models"[18,19] describe the gluon field as a classical field (contracted effectively into one dimension due to the non-abelian nature of QCD, hence "string"). Quark and antiquark represent the momentum-carrying ends of the string, and perturbative gluons are viewed as momentum concentrations, or kinks of the string[18]. In this one-dimensional color field, new quark-antiquark pairs are produced, which screen the field and recombine to form mesons (Fig. 2(c)). The modeling of the string decay closely follows the Schwinger model[20] describing charge screening in a one-dimensional world of massless fermions. The best known representative of this class is the Lund model[18,21], which employs a string decaying into mesons and baryons. The CALTECH II[22] model also uses strings, which, however, decay mainly into heavy ($\approx$ 2 GeV) hadronic clusters. Cluster decay properties are parametrized[23] based on low-energy data. Compared to QCD cluster models, string models have a few advantages: there is always the pathological case that no gluons are emitted in the perturbative phase; QCD cluster models cannot deal with such events (a 30 GeV cluster certainly does not decay isotropically!), whereas they represent no problem for string models. Furthermore, string models are manifestly infrared stable: an additional soft gluon will deflect the string infinitesimally and will not change the properties of the event. For example, a variation of the shower cutoff such that the average number of gluons per event changes from 10 to 0.1 results in a change of the average hadron multiplicity of only 10%. In cluster models, where at some point all gluons are split into $q\bar{q}$ pairs, each additional gluon - no matter how soft - increases the number of clusters by one. Of course, these arguments don't mean the string model is *right*, they just mean that string models should be more robust and require less fine tuning; the two model types represent orthogonal approximations to the properly quantized treatment of the gluon field.

3. PHENOMENOLOGICAL RELEVANCE OF PARTON SHOWERS

Let me now address the question of the phenomenological relevance of parton showers at presently available energies, as compared to fixed order calculations in perturbative QCD. There are two parts to this question, namely a) do we need parton showers to understand the structure and rates of multi-jet events, and b) is there evidence that parton showers are relevant for the phenomenology of confinement, i.e. is there any experimental evidence for the soft part of the shower, for those 5-10 gluons which will not appear as distinct jets, but should nevertheless influence the event shape?

A well known problem in the modeling of e^+e^- annihilation events is an excess of events with large aplanarity, or acoplanarity (the first quantity is a quadratic measure of the momentum flow out of the event plane, the second is linear in momentum), as compared to 2nd order QCD predictions. This is evident from the acoplanarity distribution by JADE[24] shown in Fig. 3, which is well described by the parton shower model[9] (dashed line), but not by the Lund fragmentation model using 2nd order QCD (full line). Since 3-jet events are planar, this observation points towards an underestimate of the rate of 4-jet events in the 2nd order model. This is confirmed by explicit studies of the 2,3,4, and 5-jet frequencies among events. Fig. 4 displays results of a study by JADE[24]; they use a jet finding algorithm which initially treats all particles as separate "jets", and then successively forms new jets by collapsing the two jets with the smallest invariant mass into a new jet, until the invariant mass squared M_{ij}^2 of any two jets exceeds a fraction y of the cms energy, $M_{ij}^2 > ys$. Apart from being Lorentz invariant, the algorithm also has practical advantages compared to other jet-finding techniques. The n-jet event rates are given in Fig. 4(a) as a function of y. The 2nd order QCD model underestimates the number of 4 and 5-jet events, and at the same time overestimates the number of 3 jet events, indicating that the problem cannot be solved by a readjustment of the strong coupling constant. Changes of the nonperturbative part of the model within the constraints imposed by other data don't improve the agreement either[24]. If the 2nd order QCD parton structure of the events is replaced by a parton shower, on the other hand, 4 and 5 jet rates are well reproduced. A disagreement in the 3-jet rate can be traced to the inappropriateness of the LLA in describing the first, large-angle emission of a hard gluon. The JADE analysis is now confirmed by TASSO data[25] shown in Fig. 4(b),(c); the techniques and variables used are essentially the same. However, in comparing with shower models, the TASSO group used the most recent version (6.3) of the Lund model[10,21], where the shower algorithm is patched to reproduce the $O(\alpha_s)$ result for the $q\bar{q}g$ rate exactly, yielding good agreement with the data for all jet multiplicities and for a wide range of y-values (Fig. 4 (b)) and cms energies (Fig. 4 (c)).

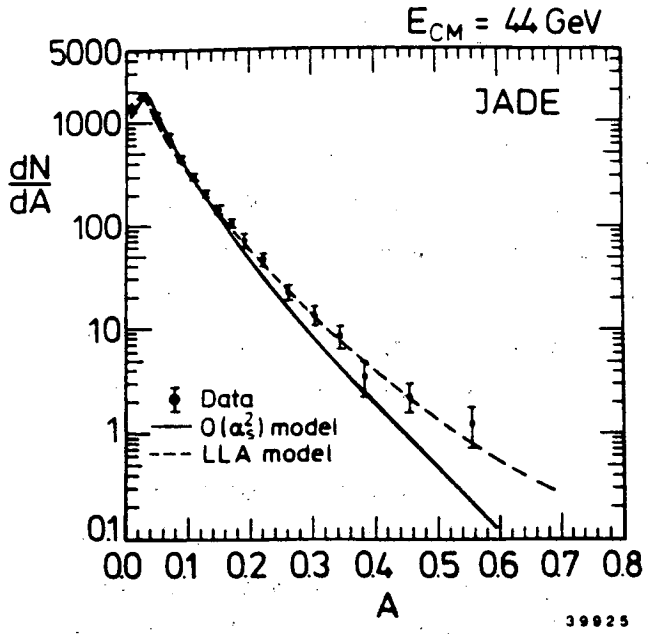

FIGURE 3

Acoplanarity distribution observed in e^+e^- annihilation at 44 GeV. Acoplanarity is defined as $4(\Sigma|p_{out}|/\Sigma|p|)^2$, where p_{out} are momentum components out of an event plane chosen to minimize the acoplanarity. Full line: Lund hadronization model using 2nd order QCD matrix elements. Dashed line: Webber hadronization model using parton shower. From JADE[24].

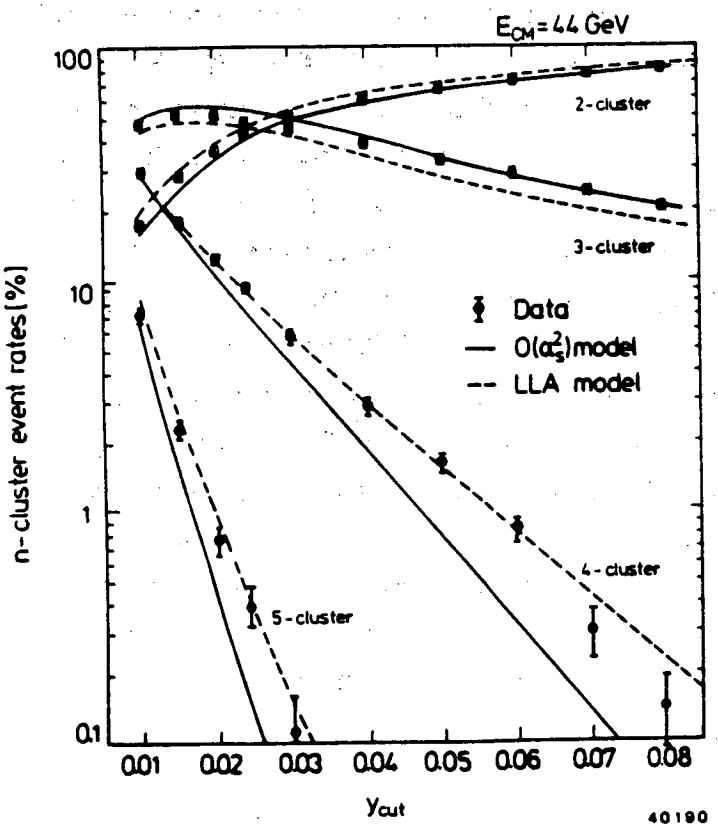

FIGURE 4

(a) Fraction of annihilation events with 2,3,4 and 5 jets (here called "clusters", but not to be confused with the color singlet clusters of QCD), as a function of the cutoff y used in the jet finding algorithm. For a given y, the invariant mass of any pair of jets has to exceed $y\sqrt{s}$. Full line: Lund hadronization model using 2nd order QCD matrix elements. Dashed line: Webber hadronization model using parton shower. From JADE[24].

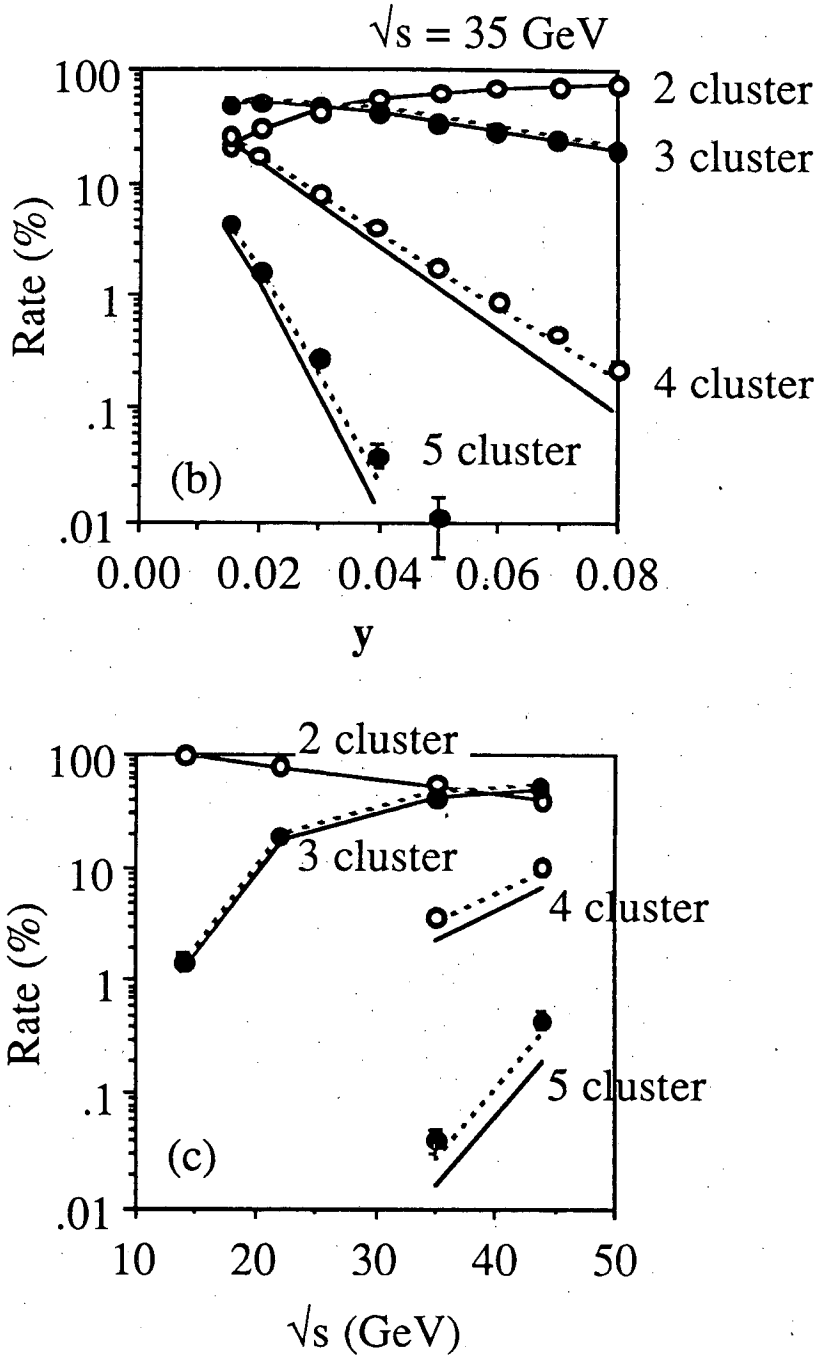

FIGURE 4(b),(c)

(b) Same as (a), but showing TASSO data. (c) Fraction of 2,3,4 and 5 jet events as a function of the cms energy, for a fixed y=0.04. Full lines in (b) and (c): Lund hadronization model using 2nd order QCD matrix elements. Dashed line: Lund hadronization model using parton shower with exact $O(a_S)$ cross section. Preliminary TASSO data[25].

Obviously, the hard part of the parton shower is needed even at PETRA energies. How about the soft, low-virtuality gluons? Let me give two examples which demonstrate the necessity to include those in the modeling, at least within the framework of the Lund hadronization model.

A first piece of evidence comes from a study of muon-nucleon scattering by the EMC group; the data has been around for a while[26] and has recently been updated[27]: Fig. 5 shows the average p_T^2 of hadrons in deep inelastic events as a function of Feynman-x, with x>0 denoting the current fragmentation region, and x<0 the target fragmentation region. Transverse momenta p_T are defined with respect to the current direction, which is determined from the change in muon momentum. As predicted qualitatively by first-order QCD[28], transverse momenta are larger in the x>0 region than in the x<0 region. However, the quantitative agreement is poor; obviously, an essential source of p_T is missing for the forward region. Adding the effects of soft gluons, which deflect the struck quark from the current direction, a much better description is obtained. The calculations shown are based on an analytical resummation of soft gluon emission[29] - a poor man's parton shower. A full shower implementation is in progress[30]. Other sources of additional transverse momentum, such as an increased nonperturbative p_T of hadrons in jets or excessive quark fermi motion in the nucleon can be excluded based on comparisons of p_T's in the current and target regions, and based on studies of p_T compensation[26,27]. We note here that despite the lower cms energy, lepton-nucleon reactions provide a more sensitive test of soft gluon effects, since the current direction is measured independently. In e^+e^- annihilation events, a jet axis has to be determined from particles in the event, reducing drastically the sensitivity to such effects.

Nevertheless, the need for the soft part of parton showers in e^+e^- annihilation is evident e.g. in a study by the TPC group[31] of pion rapidity distributions as a function of event sphericity. The basic idea is to use sphericity to select events without hard gluon activity. For the sphericity interval 0.04-0.07, e.g., one finds a rapidity distribution with a dip at $y \approx 0$, which is well reproduced by the Lund shower model, whereas the 2nd order QCD version of the model predicts a flat rapidity distribution (Fig. 6). The explanation of the dip is straightforward in the context of coherent parton showers: soft gluons are emitted at small angles, corresponding to high rapidities, and increase the particle density there. No way was found to modify the 2nd order QCD model such that it accounts for the relatively small, but significant dip.

I want to emphasize at this point that in string models that use parton showers, QCD effects can no longer be viewed as small corrections to the fundamental event structure (a straight color string). To illustrate this point, Fig. 7 depicts schematic representations of the color string(s) in individual events without QCD corrections, with 2nd order QCD matrix elements, and with parton showers. Obviously, in the latter case the differences from a simple straight string are quite drastic. (In this

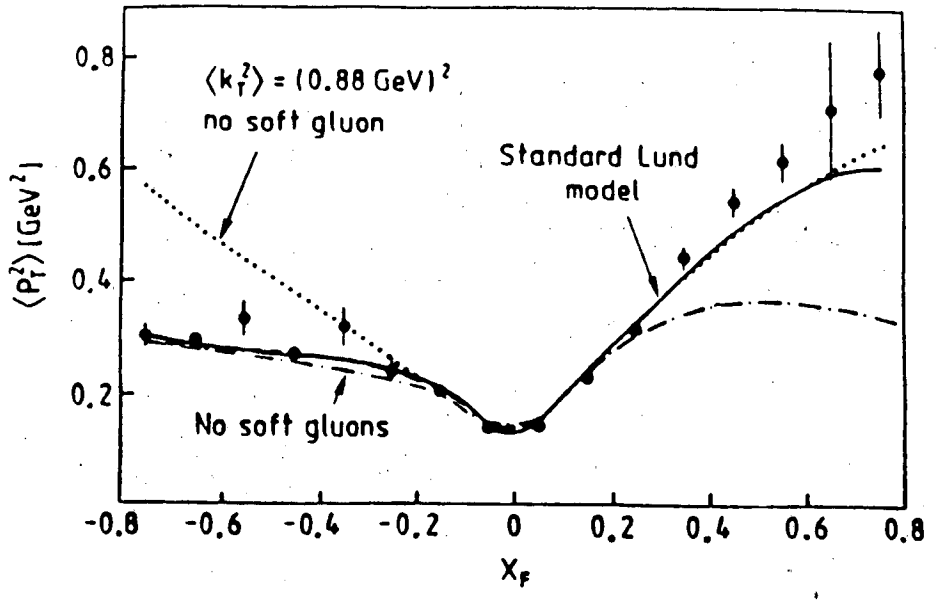

FIGURE 5

Average p_t^2 of charged hadrons produced in deep-inelastic μ-p scattering, as a function of Feynman-x. Transverse momenta p_T are measured with respect to the current direction. Full line: Lund model with 1st order hard QCD and soft gluon emission. Dashed-dotted line: without soft gluons. Dotted: without soft gluons, but increasing the primordial K_T of quarks in the nucleon from 0.44 GeV^2 to 0.88 GeV^2. From EMC[27].

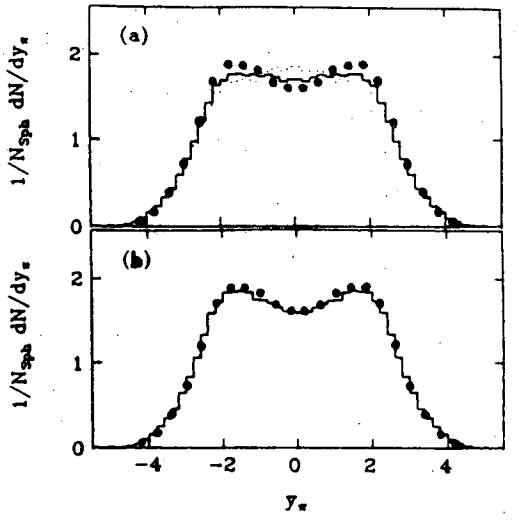

FIGURE 6

Rapidity distribution of pions in e^+e^- annihilation events at 29 GeV, for events with sphericities between 0.04 and 0.07. (a) Compared to predictions of the Lund model with 2nd order matrix elements (full line), and of an indepedent-fragmentation model, also with 2nd order matrix elements (dotted). (b) Compared to predictions of the Lund model with parton showers using a cutoff of 1 GeV^2. From TPC/2γ [31].

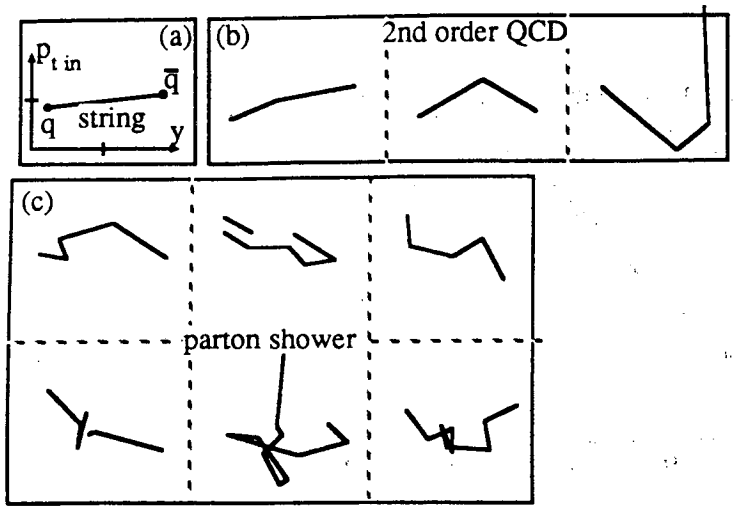

FIGURE 7

Configuration of color strings in different types of Monte-Carlo events. Parton momenta are characterized via rapidity y and transverse momentum in the event plane, p_{tin}. Color strings are indicated by straight lines joining partons. (a) a 2-jet event. (b) 2nd-order QCD events. (c) Parton shower events.

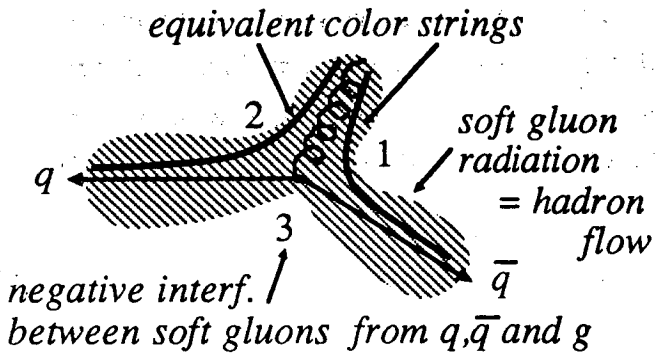

FIGURE 8

Schematic representation of the angular distribution of soft gluons in annihilation events with a hard gluon. Negative interference decreases the amount of gluon radiation into the region between q and $\bar{q}$ (region 3). The same effect is predicted in string models, where a color string is spanned from the quark via the gluon to the antiquark, thus boosting particles away from region 3, into regions 1 and 2.

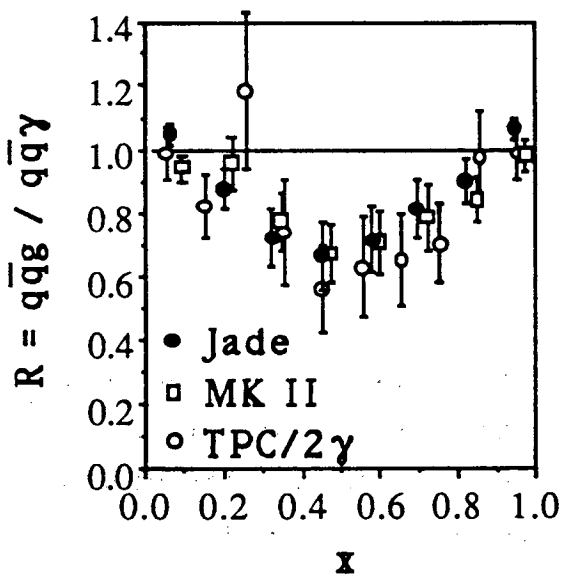

FIGURE 9

Ratio of the particle density in region 3 of three-jet events ($q\bar{q}g$) and radiative annihilation events ($q\bar{q}\gamma$), as a function of the scaled angle $x=\theta_{\text{hadron-jet}_1}/\theta_{\text{jet}_2\text{-jet}_1}$. Jets 1 and 2 of $q\bar{q}g$ events are the two highest-energy jets, typically q and $\bar{q}$. The $q\bar{q}g$ and $q\bar{q}\gamma$ events are selected to have similar kinematics, i.e. similar average momenta and angles of photon and gluon. Shown are data from JADE, MARK II and TPC/2γ [34].

context an interesting question comes up: what happens if string segments cross each other and overlap in space time? It seems unlikely that they ignore each other completely...)

4. PARTON SHOWERS AND COLOR STRINGS

The distinction between two different phases of the hadronization process - the "perturbative" and the "nonperturbative" phase - is clearly highly artificial and will have to be overcome in any real theory of parton fragmentation. Any hints for a smooth connection between the two phases, as indicated e.g. in the preconfinement phenomenon, represent steps towards a deeper understanding. A recent paper[32] can be regarded as a major milestone, since it links coherence effects in parton showers to the string model description of quark and gluon fragmentation. The authors investigate the distribution of hadrons in annihilation events with a hard gluon. They assume local duality between hadrons and partons: the angular distribution of hadrons is proportional to the distribution of soft gluons created in the shower evolution. The distribution of such gluons can be derived in analogy to a calculation of soft photon bremsstrahlung in QED; this most naive formalism breaks down for particles near the cores of jets, but should be appropriate for particle emission at large angles. In events with a hard gluon ($q\bar{q}g$), the total angular flow of soft gluons is given by a coherent superposition of soft gluons from quark, antiquark and hard gluon. The explicit calculation reveals an interesting effect: in the angular region between q and $\bar{q}$, gluon radiation from the different sources interferes destructively, resulting in a reduction of the gluon flow and hence of the hadron flow (Fig. 8). On the other hand, constructive interference takes place in the regions between quark and gluon, and between gluon and antiquark. The resulting polar pattern of the hadron flow in the $q\bar{q}g$ plane is familiar: exactly the same effect is predicted by the string model of parton fragmentation, when used e.g. with 1st order QCD (instead of parton showers): the string is spanned from the quark via the gluon to the antiquark; since each of the two string segments is moving away from the angular region between q and $\bar{q}$, this region is depleted of hadrons, which are boosted into the q-g and $\bar{q}$-g regions. In fact, the angular distribution of soft gluon radiation from the $q\bar{q}g$ system equals the angular pattern created by the incoherent superposition of hadron flows from the qg and the $\bar{q}g$ string segments in a string model, up to terms suppressed by $1/N_C$. In other words, the soft gluon interference effects provide a foundation for the string phenomenology! (The equivalence of QCD radiation and string model in the $N_C \to \infty$ limit is also evident in a number of other quantities. Consider e.g. the ratio of particle multiplicity in high-energy gluon and quark jets; this ratio is 2 in string models and $2N_C^2/(N_C^2-1)$ in QCD[1].)

Furthermore, in ref. 32 a technique is suggested to test the interference effect in a model independent fashion: one can "switch the destructive interference off" while maintaining the kinematic structure of the events simply be replacing the hard gluon by a hard photon. A comparison of the

particle flow in the region between q and $\bar{q}$ should reveal a depletion for $q\bar{q}g$ as compared to $q\bar{q}\gamma$ events. In contrast to earlier tests of the "string effect"[33] based on a comparison of particle flow in regions 2 and 3 (see Fig. 8), which are kinematically not fully equivalent, the $q\bar{q}g/q\bar{q}\gamma$ comparison can be interpreted without reference to fragmentation models. Data on the $q\bar{q}g/q\bar{q}\gamma$ comparison come from the JADE, TPC and MARK II groups[34] (Fig. 9). They plot the ratio of the angular particle flow as a function of the variable x, which maps the angular region between q and $\bar{q}$ onto the interval 0 to 1. The predicted depletion is indeed observed, and is shown to be consistent with string-model predictions (Fig. 10). The new JADE data agree well with the earlier results from the TPC and MARK II detectors.

So, string phenomenology may be understood as a convenient way to implement QCD coherence effects. This interpretation, however, raises new problems. Can we - as it is done in the Lund fragmentation model - use a coherent shower formalism and then at the end add a color string to complete the transition into hadrons, or does this result in double counting? Phrased differently: the QCD interpretation relies on the local parton-hadron duality. Strings with boost effects, however, tend to destroy this duality!

While I cannot offer a real answer to the problem, one can at least look for evidence of the potential double counting at a purely operational level. Using the ratio of hadron flow in the regions 3 and 2 (Fig. 8) as a measure for the string effect, one can ask if a model with coherent showers *and* strings predicts a larger string effect than a model based on 1st order QCD and strings, or a model based on incoherent showers and strings. The surprising answer is that coherent showers with strings, conventional showers with strings and fixed order QCD with strings predict a similar size for the string effect[7] (within non-negligible statistical and systematical errors). A likely explanation for this observation is that the short string segments between the many partons in a shower resemble in their kinematics "clusters" of the type used in QCD cluster models rather than the long (i.e. high-mass) strings required in fixed order models. As a result, the "string effect" among gluons in a coherent shower is barely enhanced in the final hadronization stage. Another indication that parton/hadron duality is indeed preserved in shower models with string hadronization comes from a comparison of the average multiplicity of partons and hadrons as a function of energy: the two multiplicities track each other within 10% over three orders of magnitude in energy (10 GeV - 10 TeV) [5].

5. A SHOOT-OUT OF FRAGMENTATION MODELS

In an attempt to identify the features required for a successful phenomenological description of parton fragmentation, the MARK II group has compared several fragmentation models with an exhaustive set of data on inclusive particle distributions and event shape variables[35]. Relevant param-

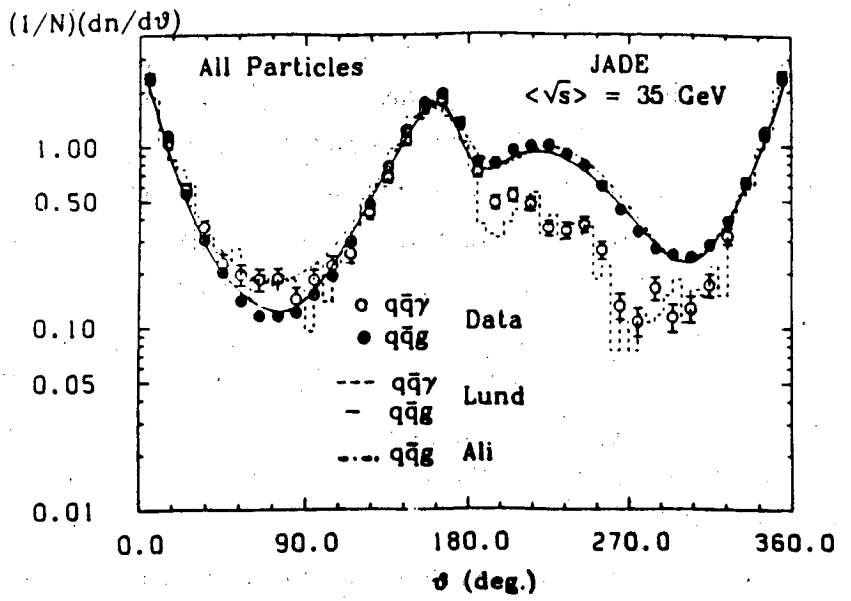

FIGURE 10

Angular flow in the event plane of particles in 3-jet events ($q\bar{q}g$) and in radiative annihilation events ($q\bar{q}\gamma$), as a function of the angle θ between a particle and the highest-momentum jet. The jet with the 2nd-highest momentum is near 160°, the third (gluon) jet or the photon is near 230°. Included are (2nd order QCD) Lund model predictions for $q\bar{q}g$ and $q\bar{q}\gamma$ and predictions of an independent-fragmentation model (Ali) for $q\bar{q}g$. From JADE[34].

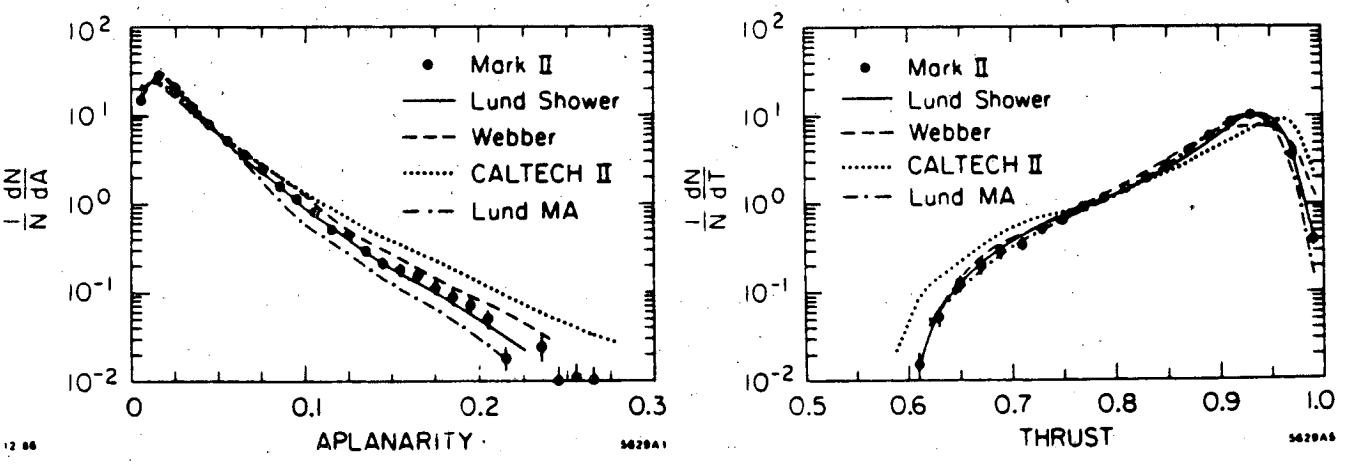

FIGURE 11

Normalized distribution in (a) aplanarity and (b) thrust of e^+e^- annihilation events at $\sqrt{s}$=29 GeV, compared to predictions of the Lund string model with parton showers (full line), the Webber model (dashed), the CALTECH II model (dotted) and the Lund model using 2nd order QCD matrix elements (dashed-dotted). From MARK II[35].

eters of the models were tuned such as to optimize the agreement with the MARK II data. (Not surprisingly, the resulting parameter values were in most cases close to their default settings supplied by the authors of the models.) Fig. 11 shows the distributions in aplanarity and thrust, compared to i) the Lund string model (version 6.3) with coherent parton showers, ii) the string model with 2nd order QCD, iii) an updated version (4.1) of the Webber[9] model, based on parton showers creating clusters and iv) the CALTECH II model[22] using a shower coupled to a string decaying into clusters. The aplanarity distribution shows once more the lack of highly aplanar events in the fixed-order model. On the other hand, the mere use of a parton shower is no guarantee for success: the CALTECH II model, and to a lesser extent the Webber model, overshoot the data for large aplanarities. Similarly, those two models fail in reproducing the thrust distribution over the full range. Compared to these event shape variables, inclusive spectra prove to be much more forgiving: for example, all models achieve a reasonable description of the distributions in momentum and in transverse momentum with respect to the jet axis. (Fig. 12; slight problems in the modeling of the large-x data above $x \approx 0.8$ should not be taken too seriously, since in this region MARK II and HRS[36] data differ somewhat). The model comparison is summarized in an overall chi-squared describing the agreement between data and model for 18 distributions with a total of 450 data points[37]. The Lund shower model emerges as a clear winner with a χ^2 of 960, followed closely by the 2nd order version with a χ^2 of 1230. This indicates that while some specific distributions show clearly the need for parton showers at PEP energies, most features of the events are still well represented by 2nd order QCD plus string fragmentation. The Webber model comes in third, with a χ^2 of 2870. The discrepancies with the data are almost entirely due to the cluster algorithm; the shower formalism of the Webber model combined with a Lund string reproduces the success of the Lund model. The situation is different for the CALTECH model: neither replacement of the shower part nor replacement of the hadronization part can reduce its high χ^2 of 6830 to competitive values.

In summary, data seem to indicate a clear preference for string models with normal mesons and baryons (instead of heavy clusters) as primary hadrons. On the other hand, it is not yet obvious if the concept of a cluster itself is at fault, or if simply the present implementations of cluster production and decay are inappropriate. An interesting by-product of the investigation is further evidence for the relevance of parton showers with very low cutoffs: the optimum cutoffs for parton virtualities are determined to be 1 GeV for the Lund model and 0.75 GeV for the Webber model!

6. THE PARTICLE COMPOSITION OF JETS

Whereas the global structure of the events is dominated by properties of the parton distribution in the events (at least at PEP/PETRA energies or above), the particle composition of the final state is mainly sensitive to the modeling of the nonperturbative phase. Measurements of the particle

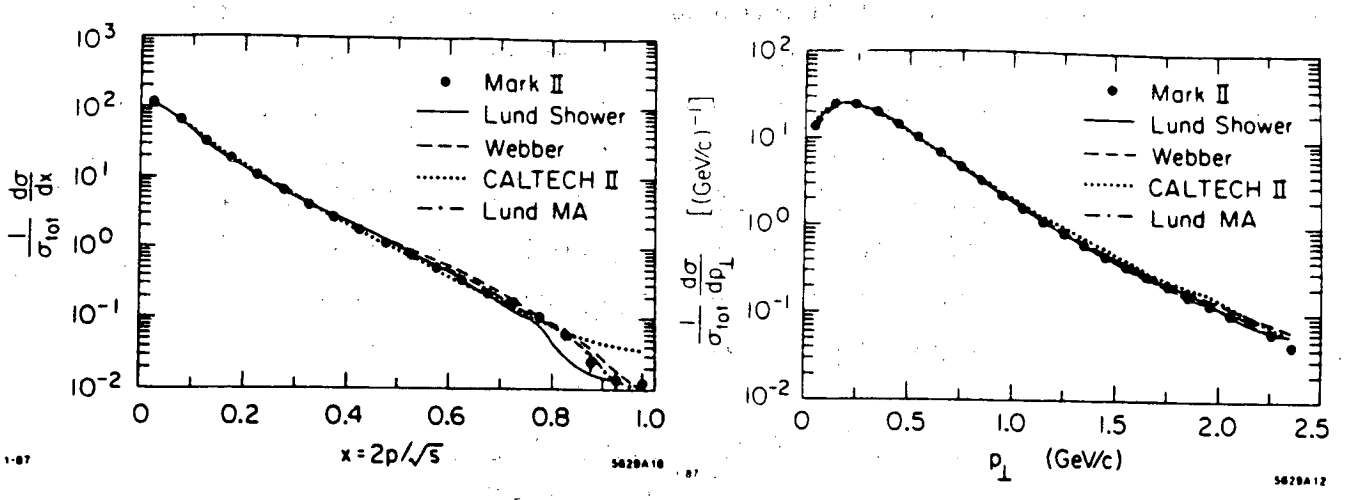

FIGURE 12

Single particle distributions in (a) $x=2p/\sqrt{s}$ and (b) transverse momentum w/r to the thrust axis, compared to model predictions (see Fig. 11). From MARK II[35].

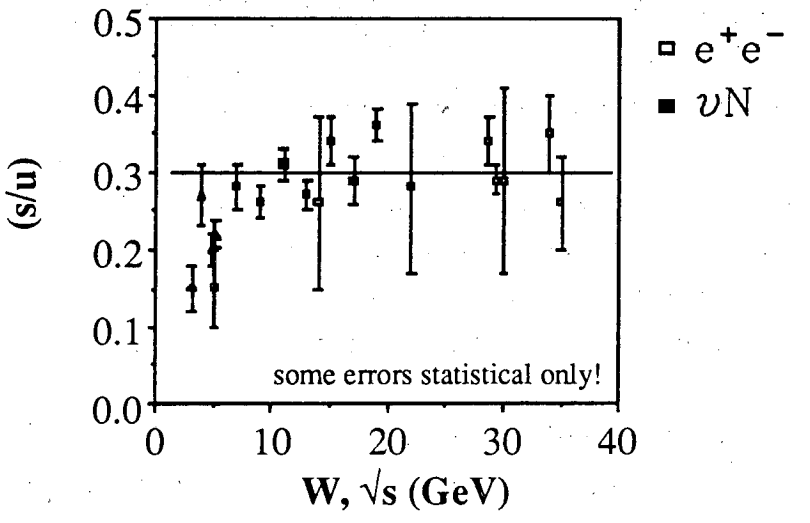

FIGURE 13

Strangeness suppression factor s/u, determined in e^+e^- annihilation and in deep inelastic lepton-nucleon scattering, as a function of the mass W of the hadronic system. Not all data points include full systematic errors[40].

composition of jets provide further constraints for models of this 2nd stage of parton fragmentation. In cluster models, the particle composition is related to the cluster mass spectrum, with the cluster decay being described by phase space or parametrized according to low-energy data. By contrast, most versions of string models put in particle composition more or less by hand via a large number of parameters, describing a) the frequencies with which different flavors of partons (light quarks, strange quarks or diquarks) are produced in the decay of the string, and b) the probabilities for two partons to recombine into different spin states. Based on world-averages of data on pseudoscalar and vector meson and on octet and decuplet baryon multiplicities in e^+e^- annihilation around 30 GeV, one finds the parameter values listed in table 1 [38] (within the Lund framework):

Table 1: Lund parameters determining particle composition

strange quark suppression	$s/u = 0.29\pm0.02$
diquark suppression	$qq/q = 0.09\pm0.01$
spin-1 diquark suppression	$\frac{1}{3}qq_1/qq_0 = 0.05\pm0.04$
extra strange diquark suppression	$(us/ud)/(s/d) = 0.7\pm0.3$
fraction of pseudoscalar mesons	
for u,d quarks	$p/(v+p) = 0.41\pm0.05$
for s quarks	$p/(v+p) = 0.45\pm0.05$
for c quarks	$p/(v+p) = 0.62\pm0.08$

Experience with different versions of string models proves that these parameters are very insensitive to the simulation of the early perturbative stages of the fragmentation process; fixed order string models and shower models use (almost) identical parameters for best agreement with the data, and predict very similar spectra (in the following, I will therefore often mention "Lund predictions" without specifying model versions etc.). The dynamics of hadron production in a color string explains qualitatively the deviations of the measured parameters from their "natural values" expected for SU(6) symmetry, such as $s/u = 1$ and $p/(v+p) = 1/4$. For example, due to the finite energy density in the string, the production of heavier quarks is suppressed[39]. The preference of pseudoscalar meson states over vector meson states (taking the spin factor into account) is simply a consequence of the lower mass of the pseudoscalars[18].

For the model to have any predictive value, it is important that these parameters are universal and roughly energy-independent. Fig. 13 proves that this is approximately fulfilled for the best-studied of these quantities, the strangeness suppression factor s/u[39,40].

New e^+e^- data submitted to this conference allow one to push the model tests further: pion, kaon and proton cross sections from the TPC detector[41] finally cover most of the kinematic range with reasonable precision (Fig. 14). In the region of overlap, the agreement with previous TPC[42] and TASSO[43] data is good. Also included in Fig. 14 are new π^0 cross sections from TASSO[44], which are in perfect agreement with the charged-pion cross sections. Lund model predictions fit the data quite well, except for the large-x proton cross sections. This is even more evident from the corresponding charged-hadron fractions shown in Fig. 15: even for large variations of the parameters it is hard to obtain perfect agreement between Lund model and data, as far as the x-dependence of the proton fraction is concerned (as of this date, however, not all possibly relevant parameters have been fully explored). On the other hand, models such as CALTECH II fail much more spectacularly. The rise of proton fractions with x in most models is caused by the treatment of baryons as being composed effectively of two constituents, a quark and a diquark, thereby treating mesons and baryons on the same footing. Kinematical effects then cause the heavier baryon to retain a larger share of the initial quarks energy. Somewhat as a surprise, proton fractions in the Webber model turn over near $x\approx0.5$ and go to zero for $x\approx1$, as predicted e.g. by dimensional counting rules[45] due to the larger number of constituents in a baryon. It is not obvious why the two cluster models - Webber and CALTECH II - behave so differently.

Also new for this conference are two detailed measurements of the inclusive η cross section. The η is interesting since in the Lund model the η production rate is closely tied to the rates of pions and kaons, the other members of the nonet; a serious failure of the model would indicate the need for even more *ad hoc* parameters, and lessen the confidence in the model's predictive power. Exactly such a failure appears to be evident from the HRS data[46]; the measured η multiplicity of 0.37 ± 0.08 is a factor two below the predictions of about 0.7-0.8 η's per event (see also Fig. 16). The HRS data and an older JADE result[47] of 0.64 ± 0.15 η's per event are marginally consistent. At the same time, however, the ARGUS group finds 0.42 ± 0.16 η's per event in their annihilation data in the continuum near $\sqrt{s}$ = 10 GeV[48], well consistent with the Lund prediction of 0.45. The comparison indicates either a completely anomalous energy dependence of η production, or a problem in one (or both) of the experimental analyses. I'm strongly inclined to believe in the latter, and comparing the quality of the η signals from the two experiments (Fig. 17), it appears somewhat premature to dig into the Lund Monte Carlo code and install and extra η suppression factor[49].

Finally, there are now e^+e^- data accumulating on mesons with orbital angular momentum. Table 2 summarizes HRS results[50] at $\sqrt{s}$ = 29 GeV, including their new K*(892) data for comparison. Also included are relevant results from the Upsilon region around 10 GeV[51].

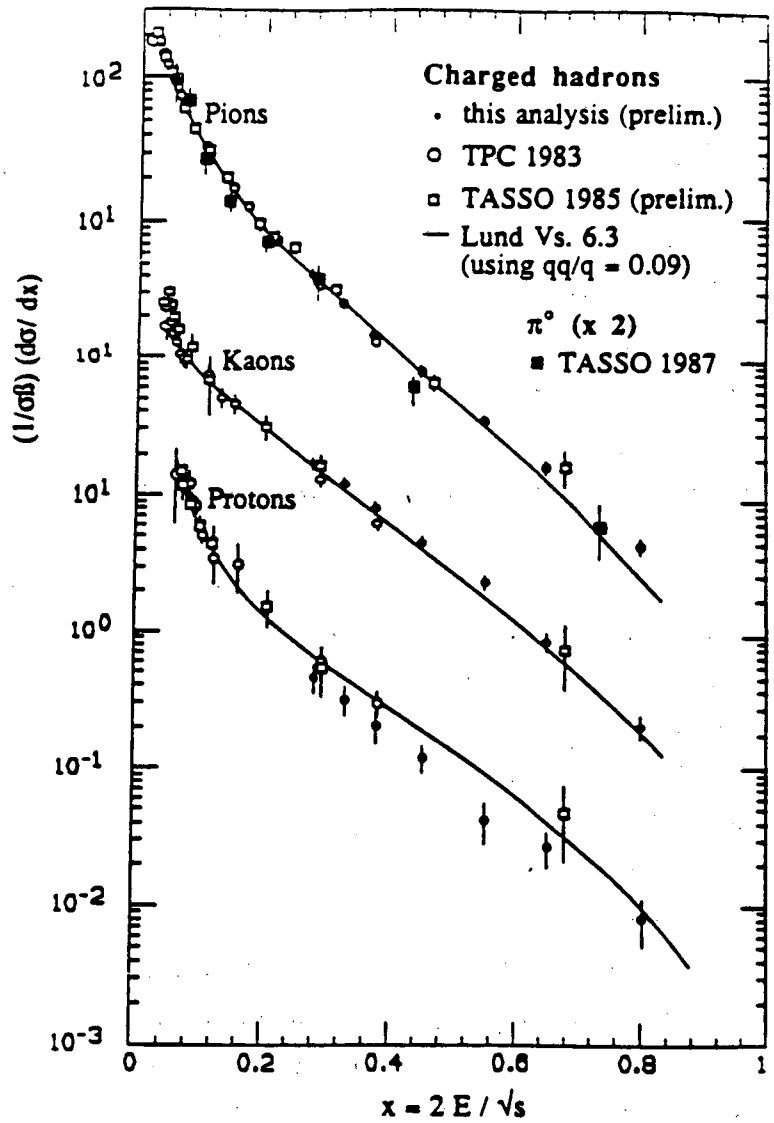

FIGURE 14

Cross section $(1/\sigma\beta)(d\sigma/dx)$ for inclusive production of pions, kaons and protons (+c.c.) in e^+e^- annihilation around $\sqrt{s}$=30 GeV, as a function of $x=2E/\sqrt{s}$. Shown are new[41] and old[42] TPC/2γ data as well as TASSO[43] data. Full lines give predictions of the Lund model (using qq/q=0.09). Also shown is a new measurement of π^0 cross sections by TASSO[44].

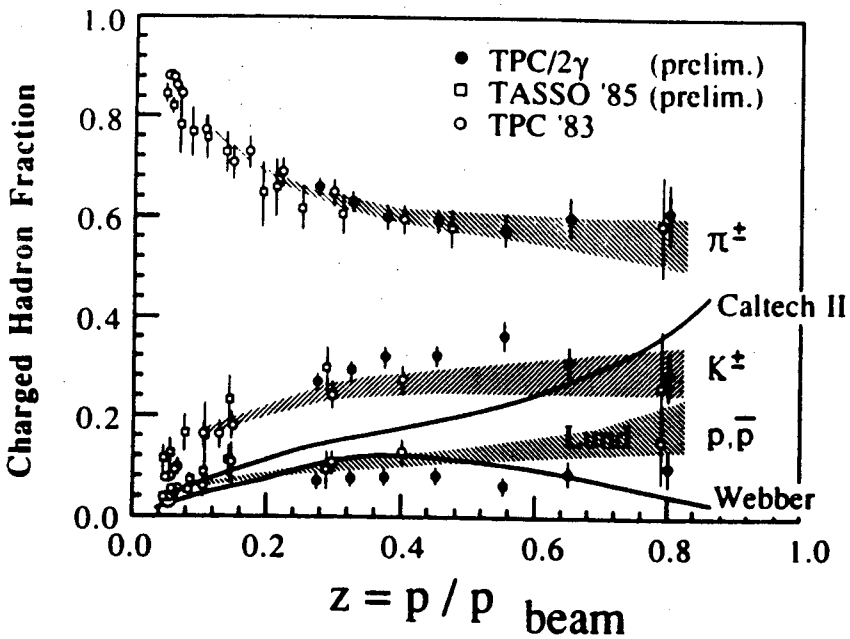

FIGURE 15

Fraction of charged pions, kaons and protons in e^+e^- annihilation around $\sqrt{s}$=30 GeV, as a function of z. Shown are new[41] and old[42] TPC/2γ data as well as TASSO[43] data. Shaded areas indicate the range of Lund model predictions for different model parameters. Also included are predictions of the Webber and CALTECH II models for the proton fraction (using default parameters).

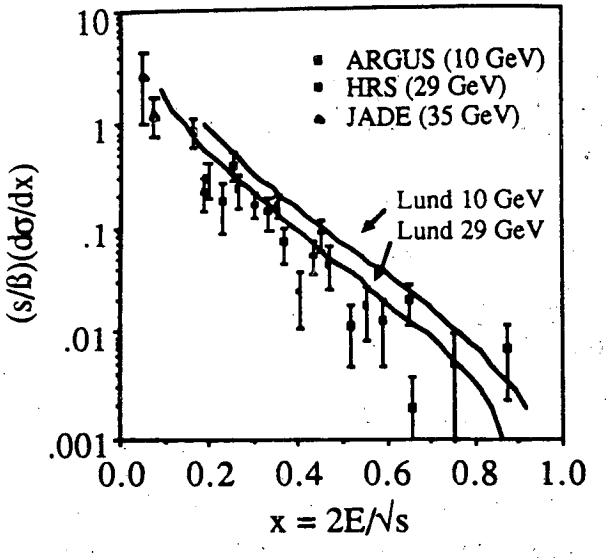

FIGURE 16

Cross section $(s/\beta)(d\sigma/dx)$ for inclusive production of eta mesons in e^+e^- annihilation at $\sqrt{s}$=29 GeV (HRS[46]), at 34 GeV (JADE[47]) and around 10 GeV (ARGUS[48]). Full lines indicate Lund model predictions for 10 and 29 GeV.

FIGURE 17

Two-photon invariant mass distributions (a) from the ARGUS experiment[48] for $0.3 < x_{\gamma\gamma} < 0.4$ and (b) from the HRS experiment[46] for $p_{\gamma\gamma} > 5$ GeV.

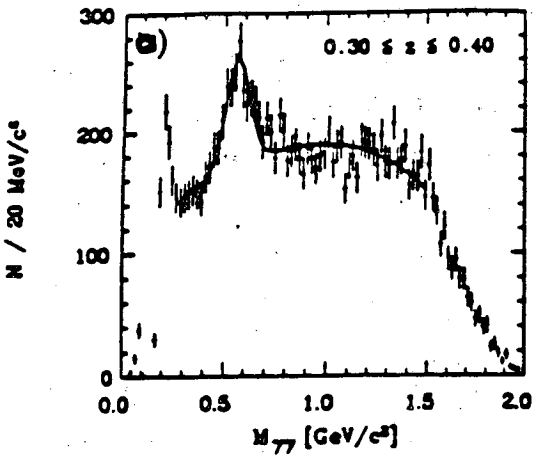

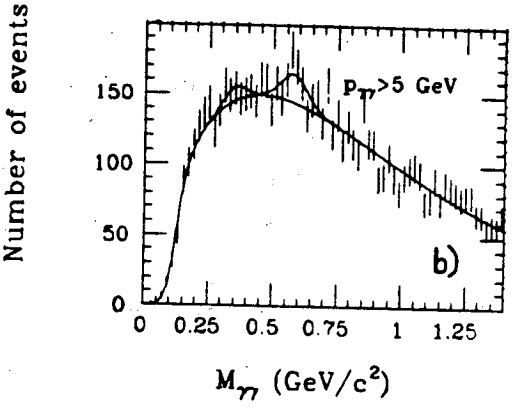

FIGURE 18

Inclusive cross section $(s/\beta)(d\sigma/dx)$ for $f_2(1270)$ and K*(1430) production in e^+e^- annihilation at $\sqrt{s}$=29 GeV, as a function of $x=2E/\sqrt{s}$. Lines indicate predictions of the Webber model. From HRS[50].

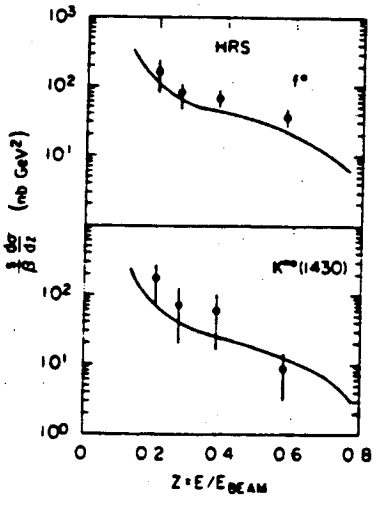

Table 2: Inclusive rates for l=1 mesons

Meson	J^{PC}	Rate/event	Ref.
$f_2(1270)$	2^{++}	0.14±0.04	HRS
$K^{*\pm}(1430)$	2^{+}	0.09±0.03	HRS
$K^{*\pm}(1430)$	2^{+}	0.12±0.06	HRS
$f_0(975)$	0^{++}	0.06±0.03	HRS
$D^{*0}(2420)/D^{*+}$		0.17±0.09	ARGUS
$D^{*0}(2420)/D^{*+}$		0.12±0.05	CLEO

Typical rates for L=1 mesons are around 0.1 per event, corresponding to 10-20% of the production rate for vector mesons. A similar ratio is obtained for charmed mesons. This seems to imply that L=1 mesons are not a dominant source of stable hadrons; only 7% of all kaons originate from K*(1430), compared to 42% from K*(892). The fact that L=1 meson production is neglected e.g. in the Lund model should hence not cause major problems. The K*(1430) to K*(892) ratio can be understood qualitatively both in the string framework (with about 1 fm between string breaks and typical transverse momenta around 300 MeV it is easy to create one unit of orbital angular momentum, but the L=1 wave function disfavors quark recombination into such states), and within the cluster framework, where heavy mesons are suppressed by phase space (Fig. 18).

7. BARYON PRODUCTION IN JETS

While detailed data on inclusive meson cross sections and particle composition certainly provides valuable constraints and guidelines for the construction of fragmentation models, it is often hard to find the relation to the underlying physics, mainly since virtually nothing can be derived from first principles and since there are usually many parameters and effects which influence any given distribution[52]. A more powerful tool may be the study of baryon production, which offers several interesting features:

- As evidenced in Fig. 15, models differ widely in their predictions for baryon rates, much more than in the meson sector.
- Baryons provide a more direct probe of the confinement process. Most pions are created in resonance decays, rather than as primary hadrons during the color confinement. As a result, the reconstruction of the primary production process using final pions is a difficult task. For example, the rms rapidity difference between a pion and its first-generation ancestor is about 0.5 units, comparable to the length of typical rapidity correlations. Protons, on the other hand, are directly produced in more than 50% of the cases, and have an rms rapidity difference to their ancestor of

only 0.08 units, thus preserving all primary correlations. (The numbers given here refer to the Lund model; however, the qualitative arguments hold independently of details of the modeling.)

- Finally, the possibility to vary the number of strange quarks in a baryon between 0 and 3 provides an improved lever arm for studies of the flavor dependence of cross sections.

The second point given above also applies to heavier mesons; however, those cannot be identified with sufficient purity to go beyond inclusive studies.

Before using baryon spectra and correlations between baryons to study confinement, one needs to demonstrate that baryons are indeed a direct product of the hadronization process, and not just decay products of heavy meson-like states, as proposed e.g. in early versions of the Webber model. Relevant data was published by the TPC group[53], and is now available with significantly improved statistics. The analysis uses events with at least one proton and one antiproton; Fig. 19 shows the distribution in $|\cos\theta|$ for these pairs, after subtraction of random combinations. Here θ is the angle between proton momentum and jet axis, measured in the p-$\bar{p}$ rest frame. Baryons from meson decay should yield a flat distribution in $|\cos\theta|$, quite in contrast with the experimental data, which is peaked near $|\cos\theta|\approx 1$ and proves that baryons are sensitive to the direction of the initial color field and are therefore produced during and not after the confinement process.

The same data set has been used to study rapidity correlations between baryons[54]. Among the results is further evidence for the local conservation of baryon number: the net excess of baryon number per unit rapidity in events with a "trigger" antibaryon at a given fixed rapidity peaks at the rapidity of the trigger particle. Examples for a trigger-$\bar{p}$ around $y\approx 0.6$ and for a trigger-$\bar{\Lambda}$ near $y\approx 1.3$ are shown in Fig. 20(a) and (b). Local conservation of baryon number is expected in most fragmentation models; a more interesting feature shows up in rapidity correlations between two antiprotons[55] or between an antiproton and an antilambda (Fig. 21). The correlation function C is defined as usual:

$$C = \left(\frac{1}{\sigma}\frac{d^2\sigma}{dy_a dy_b}\right) \Big/ \left(\frac{1}{\sigma^2}\frac{d\sigma}{dy_a}\frac{d\sigma}{dy_b}\right) - 1$$

This definition yields C=0 for uncorrelated production obeying Poisson statistics. Like in Fig. 20, one $\bar{p}$ is fixed near $y_a\approx 0.6$ and C is displayed as a function of the rapidity y_b of the other antibaryon. We observe a large negative correlation between antibaryons of similar rapidity or, in other words, a "repulsion" between two antibaryons. The range of the effect for $\bar{p}\bar{p}$ is far too big to be attributed to Fermi-Dirac statistics, assuming usual source sizes of about 1 fm. The phenomenon is reproduced by the late versions of the Lund model ("symmetric Lund"), whereas earlier versions ("standard Lund") or the Feynman-Field (FF) model (upgraded to include baryon production[56]) fail to describe the data. The lesson to be learned is simple: particle production is usually pictured as a chain of new quark-antiquark pairs spanned between the initial quarks (Fig. 22(a)). The standard

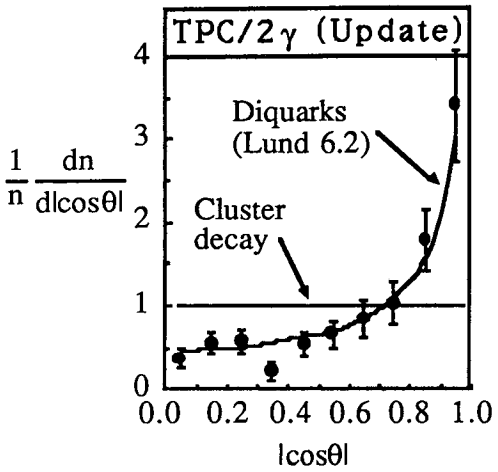

FIGURE 19

Distribution in $|\cos\theta|$ of proton-antiproton pairs produced in in e^+e^- annihilation at $\sqrt{s}$=29 GeV, after background subtraction. θ is the angle between the proton momentum and the jet axis, measured in the proton-antiproton rest frame. Lines give model predictions for proton production via a diquark mechanism and via cluster decay. From TPC/2γ.

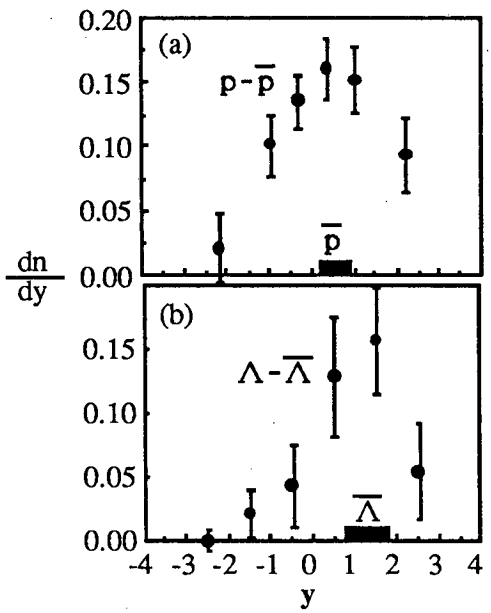

FIGURE 20

(a) Net baryon number density observed in e^+e^- annihilation events with an antiproton near y≈0.6. The baryon number density is defined as the number of protons per event and unit rapidity minus the number of antiprotons. (b) As (a), but using lambdas, and for a higher rapidity y≈1.3 of the "trigger"-antilambda. From TPC/2γ [54].

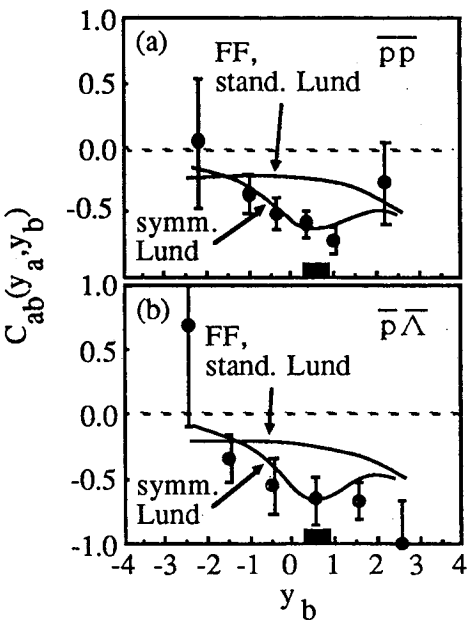

FIGURE 21

(a) Correlation function between an antiproton at y_a≈0.6 and another antiproton at y_b, as a function of y_b. Lines show predictions of the Lund model using the symmetric fragmentation function and using Feynman-Field or standard Lund fragmentation functions. (b) as (a), but showing the correlation between an antiproton at y_a≈0.6 and an antilambda at y_b. From TPC/2γ [54].

(and so far only successful) implementation of baryon production is via occasional production of diquark-antidiquark pairs[57]; natural mechanisms to achieve this have been described e.g. in ref.[58]. Obviously, quantum numbers such as charge, strangeness or baryon number will alternate along the chain; it is impossible for two neighboring particles to have the same (non-zero) charge, strangeness or baryon number. Provided that rapidity y and rank in the chain are closely correlated, this would explain the anticorrelation between two antibaryons. The mapping between rank and rapidity is governed by the function f(z) which (in an iterative implementation) determines which fraction of the available energy goes into the next hadron[18,59]. Both the "standard" Lund model and the FF model use f(z)'s which peak at z=0 (Fig. 22(b)). This means that it is likely that a hadron receives a very small energy fraction, leaving a lot for the remainder of the chain and making it not too unlikely that a later hadron will obtain more energy and end up at a higher rapidity. In other words, the correspondence between rank in the chain and rapidity is rather poor. This changes for the "symmetric" Lund model, with $f(z) = \frac{(1-z)^a}{z} e^{-bm^2/z}$. In particular for heavy hadrons, this function exhibits a pronounced peak at intermediate z and goes to zero for small z. Such an f(z) tends to give each (heavy) hadron an almost fixed fraction of the available energy, resulting in a tight correlation between rank and rapidity, and in an anticorrelation between particles with identical (charge-like) quantum numbers. The effect is invisible for pions, since for small masses the symmetric f(z) also peaks near z=0 and is similar in shape to the function used in the "standard" Lund model, and since resonance decays and Bose-Einstein enhancements cover the anticorrelation further. In conclusion, the observed effect provides strong support for the "symmetric" fragmentation function derived by the Lund group[60] and others[61].

I would like to mention a way to visualize the mechanisms by which the reordering of particles is suppressed in a proper string picture. Fig. 23 shows the space-time evolution of particle production by a color string. The square of the matrix element for production of a given final state[18,19] is proportional to e^{-bA}, where A is the space-time area swept by the color field and b is a constant. This area law results from the fixed probability per unit length and time to break the string by quark pair production. For the diagram of Fig. 23(a), the order in rapidity of the hadrons h_1 and h_2 corresponds to their order in rank; note that hadron momenta are determined by the production points of their constituent quarks. If the rapidity order is reversed (Fig. 23(b)), the area of the color field is increased and hence the production probability is strongly suppressed.

8. FLAVOR DEPENDENCE OF BARYON RATES

I will now turn to the dependence of inclusive baryon production rates on the quantum numbers of the baryon. New data submitted to this conference include Ξ^- spectra and a limit on Ξ^{*0} pro-

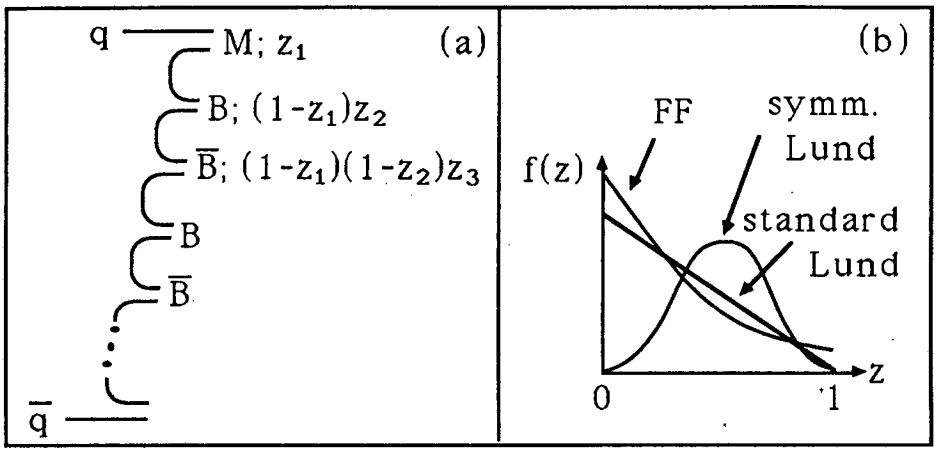

FIGURE 22

(a) Hadronization chain resulting in the production of two baryons and two antibaryons. (b) Fragmentation function f(z) describing the energy sharing between hadron H and remaining parton (quark or diquark) p' in the basic process $p \rightarrow H(z)+p'(1-z)$ in iterative fragmentation models, for the symmetric Lund, standard Lund, and Feynman-Field models.

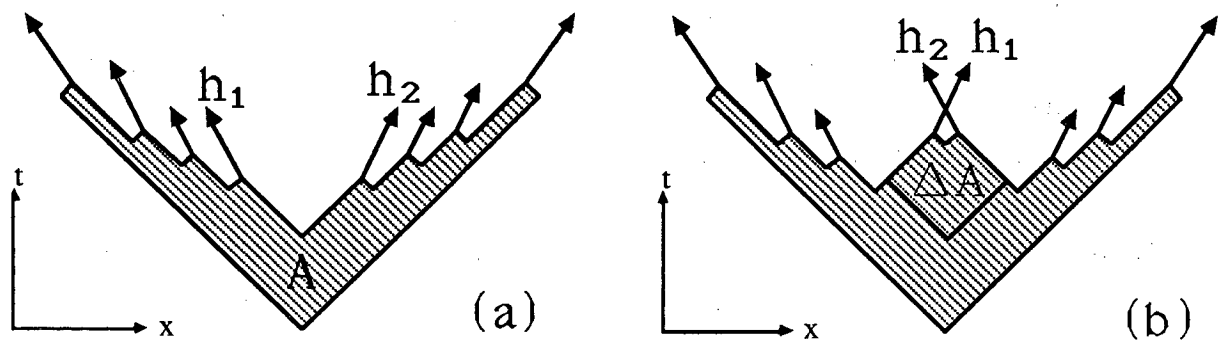

FIGURE 23

(a) Space-time diagram of hadron production in string models. The ordering in rapidity of the central two hadrons h_1 and h_2 corresponds to their order in rank along the fragmentation chain. (b) Effect of reversal of the rapidity order of h_1 and h_2 on the space-time area swept by the string.

duction in e^+e^- annihilation at 29 GeV from the MARK II[62], corresponding data on $\Sigma^{*\pm}$ and Ξ^- from the HRS[63], and results from the ARGUS collaboration on Λ, Σ^o, Ξ^-, Σ^{*+}, Σ^{*-}, Ξ^{*o}, Ω^- and $\Lambda(1520)$ production in the e^+e^- continuum around 10 GeV and on the Y resonances[64]. Instead of discussing individual cross sections, let us investigate the dependence of cross section on the number of strange quarks in a baryon by forming cross section ratios for members of the same multiplet, such that the particle in the numerator has one additional strange quark compared to the particle in the denominator (Fig. 24, including previous results[65,66]). With the exception of one CLEO point, we find good agreement within experiments. The additional strange quark causes a reduction of the rates by about 0.3, as seen for the heavier baryons which are dominantly directly produced (as compared to Λ and p, where rates are dominated by feeddown from decays). Also included in Fig. 24 are bands corresponding to predictions of the Lund, Webber and CALTECH II Monte Carlos at 10 GeV cms energy. The Lund model describes the data reasonably well, whereas the Webber model is systematically somewhat high, indicating that the suppression of strange baryons due to cluster decay phase space alone might not be sufficient. The CALTECH II model underpredicts most ratios. The distinction between models is more obvious from at the spin-dependence of cross sections: Fig. 25(a) shows ratios of decuplet and octet production rates of baryons with the same number of strange quarks. A strong suppression of decuplet particles is obvious, even allowing for the feeddown, which is not corrected for. Comparison with Webber model predictions demonstrates once more the existence of dynamical suppression mechanisms beyond cluster decay phase space. It is also interesting to notice that $\sigma_{\Lambda(1520)}/\sigma_{\Sigma^*} > 1$ (Fig. 25(b)), i.e. that it is more difficult to make three quark spins line up than to create a unit of orbital angular momentum.

One can try to describe the baryon rates quantitatively using a diquark model based on SU(6) symmetry broken by suppression factors for different quark and diquark flavors[66]. The model (which neglects leading-quark effects) reproduces the data very well using the following suppression factors:

Table 3: Fitted Quark and Diquark Suppression Factors

Quarks	s/u	0.2 - 0.3
Spin-0 diquarks	us_0/ud_0	0.07±0.03
Spin-1 diquarks	ud_1/ud_0	0.01±0.02
	us_1/ud_0	0.007±0.003
	ss_1/ud_0	0.002±0.001

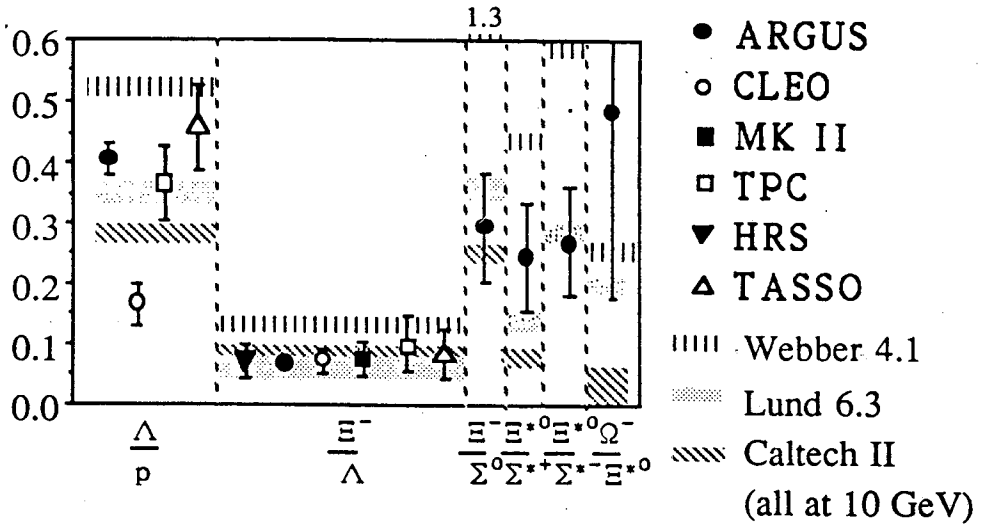

FIGURE 24

Strangeness suppression in baryon production. Shown are ratios of baryon production cross sections for strangeness s+1 and s (s=0,1,2), for baryons belonging to the same spin multiplet. Feeddown due to decays is not corrected and affects mainly p and Λ rates. Data from e^+e^- annihilation in the continuum near $\sqrt{s}$=10 GeV from ARGUS and CLEO, and around $\sqrt{s}$=30 GeV from MARK II, TPC/2γ, HRS and TASSO[62-66]. Shaded bands represent predictions of the Lund, Webber and CALTEC II models (for $\sqrt{s}$=10 GeV).

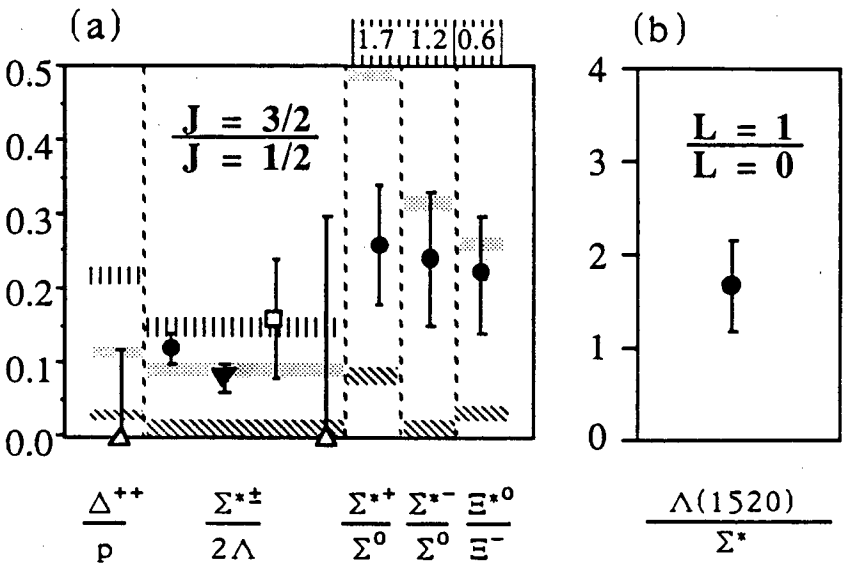

FIGURE 25

(a) Ratios of inclusive production rates for decuplet and octet baryons. Only baryons with the same strangeness content are compared. See Fig. 24 for explanation of symbols. (b) Ratio of Λ(1520) (J=3/2,L=1) and Σ^*(J=3/2,L=0) production rates, as measured by ARGUS[64].

The strong suppression of heavy (i.e. strange) diquarks and of spin-1 diquarks lends strong support to diquark models, where these effects are predicted. The strange diquark suppression factor agrees with earlier results from the TPC[67] and EMC[68] groups. However, the HRS group obtains a strange diquark suppression comparable to the strange quark suppression[69] and points out that the value of this parameter is strongly correlated with the values for charmed baryon branching fractions into Λ+x assumed in the analysis. This uncertainty does not enter into the EMC analysis, though. At least for the PEP and PETRA data, refinements in data and analysis techniques are required to solve this question.

9. GLUON FRAGMENTATION

Gluon fragmentation provides a further test of our understanding of the perturbative and non-perturbative mechanisms of jet evolution. In particular, gluon jets are predicted[1,70] to have a softer particle spectrum than quark jets. First data confirming this was shown by the MARK II group about two years ago[71]; further evidence was recently published by the UA1 collaboration[72] (Fig. 26).

Several experiments studied the transverse width of gluon jets. From the UA1 data, a ratio of the average transverse momenta of hadrons in quark and gluon jets was derived to 1.03±0.22. A similar result - identical transverse momenta for the two types of jets - was submitted to this conference by the CELLO group[73]; they compare the 3rd (lowest-energy) jet in three-jet events at 35 GeV cms energy with a reference (quark) jet at 14 GeV cms energy and find $\langle p_T \rangle_{3rd\ jet}/\langle p_T \rangle_{ref\ jet}$ = 1.03±0.05. I should comment here on a common misconception: QCD does not predict larger transverse momenta for gluon jets; it predicts larger opening angles, basically a reflection of a softer hadron spectrum and a constant p_T scale. At high energies, phase space constraints in gluon jets actually result in a slightly lower average p_T. At low energies (i.e. for gluon jets at PEP or PETRA), the string effect (see above) may make gluon jets slightly wider in cross section and also sightly oblate. The CELLO group has looked for the latter effect and finds a null result comparing the transverse momentum components in and out of the event plane for the lowest-energy jet in 3-jet events: $\langle p_{T\ in} \rangle/\langle p_{T\ out} \rangle$ = 1.02±0.06. This result is however still consistent with string model predictions of 1.08±0.02.

A drastic difference in the particle composition of quark and gluon jets has been known for a while, and has now been studied in great detail by the ARGUS group[64]: the enhanced baryon production in Y decays into 3 gluons ("Y direct") as compared to the nearby continuum. The averaged data from ARGUS[64] and CLEO[65] is displayed in Fig. 27. Meson multiplicities on and off the Upsilon are similar, whereas baryon production on the Upsilon is enhanced by factors of order 2 to 3. Only $\Lambda(1520)$ rates are not significantly enhanced. No enhancement is observed for the ϕ, ruling

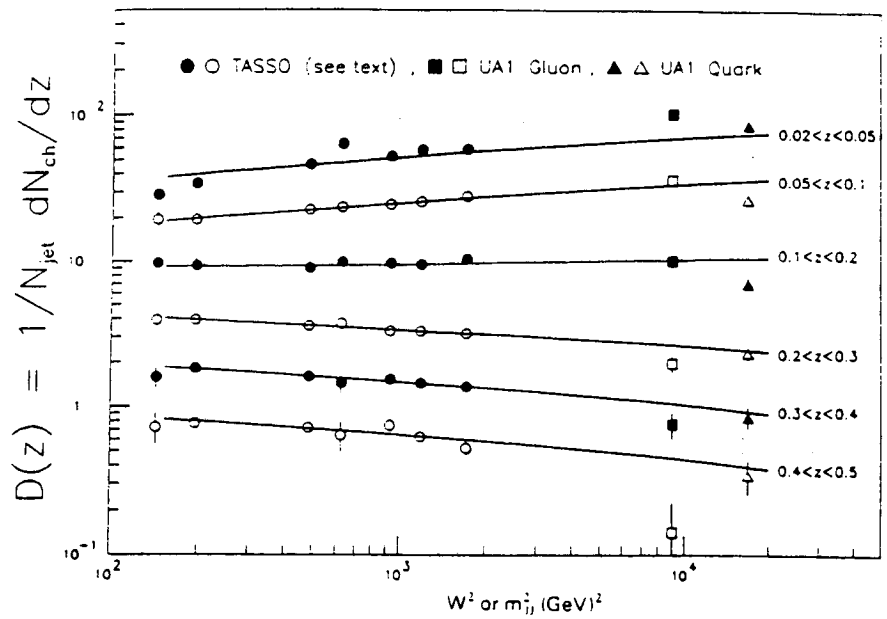

FIGURE 26

Fragmentation function D(z) as a function of the jet-jet invariant mass W, for different z bins. Shown are quark-jet results from TASSO and UA1, and gluon-jet results from UA1. In the UA1 analysis[72], quark jet and gluon jet enriched samples are selected based on the kinematics of the hard scattering process and the resulting x values of the interacting partons.

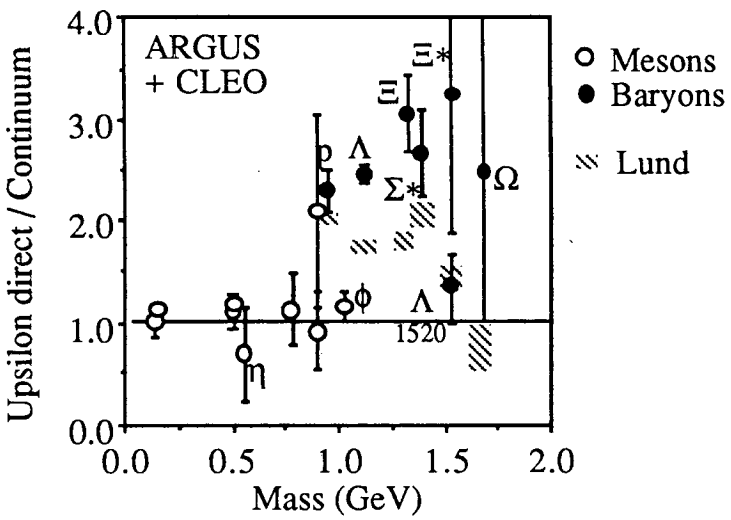

FIGURE 27

Ratio of particle production rates in three-gluon decays of the Upsilon(1s) and in the nearby continuum, for mesons (open circles) and baryons (closed circles) as a function of hadron mass. Data points combine ARGUS[64] and CLEO[65] data, where available. Shaded bands represent Lund model predictions.

out of pure mass dependence of the effect (protons are enhanced by factors >2), as expected e.g. in the Field model[74]. We note in passing that the absence of an enhancement of inclusive η rates rules out the "leading isoscalar" model[75], according to which a leading particle in a gluon jet should be an isoscalar.

The baryon enhancement can be understood qualitatively in the Lund model (Fig. 27); the model does not achieve a quantitative description, however. In the string model, the baryon enhancement is created as follows: in the continuum, leading hadrons (i.e. those containing the initial quarks) have a smaller chance of materializing as a baryon than leading hadrons in gluon jets: for the former, one constituent is known to be a quark whereas in the latter case both constituents are newly created and either of them could be a diquark, roughly doubling the chances for baryon production[58]. The hypothesis could be tested[76] by selecting only non-leading (i.e. central) hadrons in continuum events. However, at only 10 GeV cms energy such a selection is difficult, and the high-energy data lack statistics. It is also worth noting that in this model as well as in most others suggested to explain the effect, the baryon enhancement is a low energy effect and should disappear at higher energies.

10. STRING MODELS: NEW IDEAS

The color string model of parton fragmentation is highly successful and has proven a fertile ground for extensions, which may ultimately eliminate some of the problems with the model such as the ever increasing number of parameters or the doubts concerning double counting when a string is used together with parton showers. I will discuss in detail one recent modification of the Lund string model and mention some others.

As discussed before, the production of hadrons is basically described as a two-step process: quark production followed by recombination into hadrons. Parton production and particle composition are governed by *ad hoc* parameters, whereas the momentum distributions are given by the mass-dependent symmetric fragmentation function $f(z,m) = \frac{(1-z)^a}{z} e^{-bm_T^2/z}$ discussed in connection with the baryon correlations. The $(1-z)^a$ term reflects longitudinal phase space, whereas the exponential term reflects the area law discussed above (Fig. 23). Given that quark production and recombination involve similar time scales, and that in a quantum mechanical description of the process the production probability of a given quark will depend on its future - e.g. on the wave function of the bound state - one may try the alternative approach of a string coupling directly to hadrons. The basic idea is illustrated in Fig. 28, which shows the usual space-time diagram describing quark pair production in the string, propagation of quarks until they meet a partner, and then propagation in a "yoyo" mode as a bound meson (Fig. 28(a)). Equally well, one can however

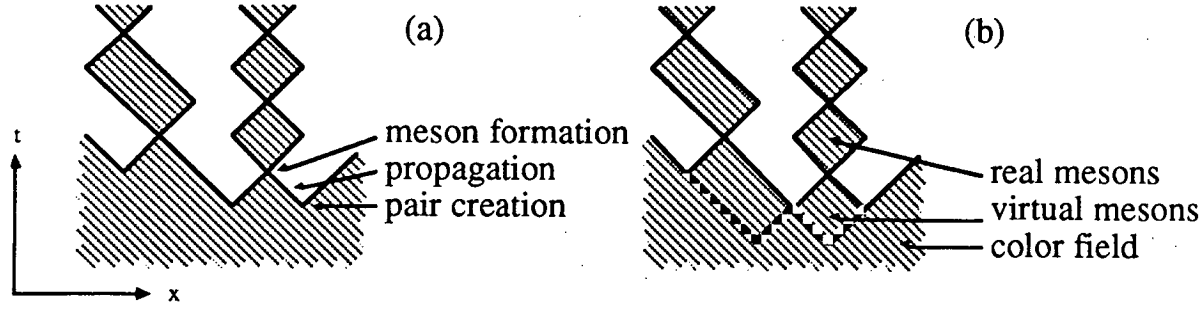

FIGURE 28

Space-time diagrams describing hadron production in string models: (a) conventional formulation based on the string -> quarks, quarks -> mesons transition in a one-dimensional system of massless quarks and (b) alternative description as a direct transition string -> mesons.

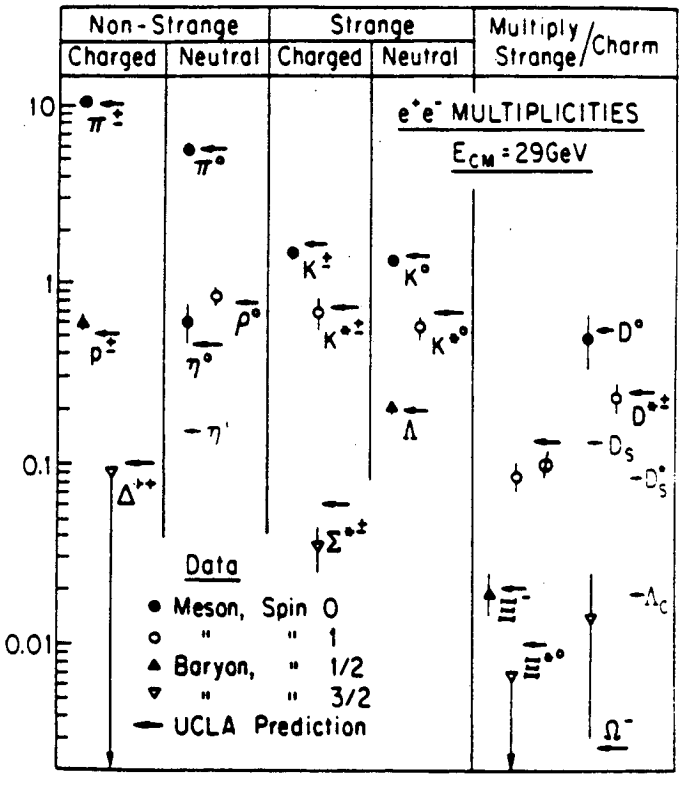

FIGURE 29

Predictions of the UCLA model[38] for hadron production rates in e^+e^- annihilation at $\sqrt{s}$=29 GeV (arrows), compared to experimental data (averaged over detectors, where available). The two model parameters a and b are tuned for optimum agreement with the data, resulting in a=1.1 and b=0.75 GeV^{-2} (in the Lund Vs. 6.2 framework).

view the stage of propagation of the quark as part of the first oscillation of the meson "yoyo" (Fig. 28(b)); from this point of view it appears that the color flux tube as a whole undergoes a transition into meson states, without an intermediate quark stage. Of course, due to the uncertainty relation the two views cannot really be distinguished, but the question remains as to which (if any) is the more appropriate classical analogue.

In the framework of Fig. 28(b), only the hadron mass is left as a quantity to govern cross sections. One might speculate that the fragmentation function given above describes not only the x distribution for a given hadron flavor and given p_T, but that it also governs, via the (transverse) mass dependence, the particle composition[38] and the transverse spectra[38,77]. The two parameters a and b (instead of the usual dozen parameters) account then for the suppression of large transverse momenta, of vector mesons, of strange mesons and of baryons. Such a modification of the Lund string model has been studied in Ref. 38. More or less by construction, this ("UCLA"-)model retains inclusive distributions predicted by the Lund model. Amazingly enough, it predicts hadron rates for non-strange and strange mesons and baryons correctly within about 30-40%, over a range of more than 3 orders in magnitude between common (π) and very rare (Ω) particles (Fig. 29). Transverse-momentum spectra are also reproduced well. While there are certainly open questions as to the details of the implementation of this model, it demonstrates that present data cannot be used to prove conclusively that the suppression of strange hadrons and baryons actually occurs at the quark level. Much more precise measurements of production rates are needed for a better distinction!

Another extension of the basic string model concerns effects of quantum statistics. As is well known, identical bosons exhibit Bose-Einstein correlations[78], i.e. the emission of n identical particles in the same quantum state is enhanced by n!. So far, models based on a stochastic fragmentation process fail to account for this effect. The fundamental area law of string models can be exploited to include such quantum effects in the Lund model, and thereby bring it a step closer to a reality. After identifying the e^{-bA} term in the production probability with the square of a matrix element, one can guess the phase $e^{-i\kappa A}$ of the production amplitude for a given final state from the analogy to Wilson loops[79] or simply from the classical string action[80]. ($\kappa \approx 1$ GeV/fm is the string tension.) Given the complete amplitude, it is straightforward to sum over all permutations of identical particles and to derive from the square of the amplitude sum a weighting factor for Monte Carlo generated events, whose distribution is originally determined by the sum of squares of amplitudes. Pending some complications due to resonance decays, such a modified string model[81] accounts quite well for the observed interference phenomena[79,81] (Fig. 30).

Finally, I want to mention a model which departs from the classical technique to use perturbative QCD to describe the event structure: Andersson et al. have proposed[82] a probability measure for a string configuration, which at no point refers to classical perturbative QCD. They observe that

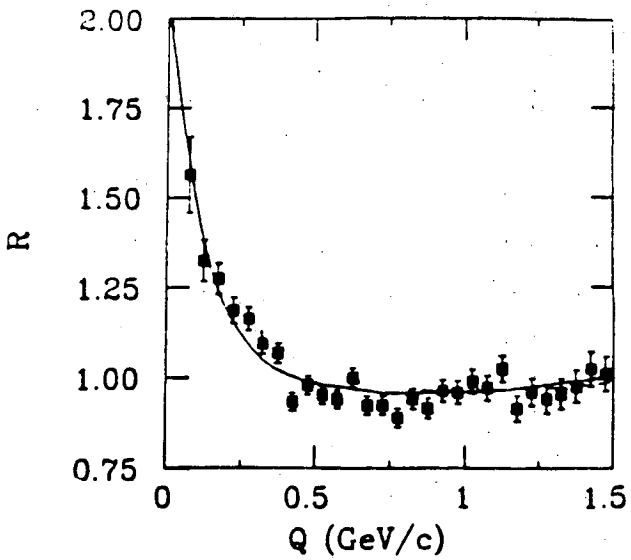

FIGURE 30

Experimental two-pion correlation function R as a function of the four-momentum transfer Q, from e^+e^- annihilation events at 29 GeV. Solid curve: string model prediction for primary pions[79].

the probability to find a string segment is $P \sim e^{-bA}$ (up to log. corrections), where A is again the space-time area swept by the string. In an annihilation event, the string can take numerous shapes, which can be approximated by straight pieces of string between kinks of the string. The dynamical mechanism to create such a string is of course a parton shower. However, instead of referring to the shower evolution, one can now describe the probability for a given string configuration simply as a product of a phase space factor (which favors strings with many kinks) and the e^{-bA} factor, which is largest for straight strings. The model reproduces the leading poles of QCD, but gives different results for the particle flow at large angles with respect to the jet axes. Since the model uses the string language consistently, questions concerning double counting etc. never appear! Unfortunately, problems in the actual implementation of these ideas in a Monte Carlo generator have slowed down developments in this direction.

11. SUMMARY

While the study of the physics of jets during the last years has not given rise to revolutions in our understanding of the strong interaction, it is certainly characterized by a steady and evolutionary progress.

Even at PEP and PETRA energies, we find evidence for QCD effects beyond the 2nd order calculations, and see the effects of parton showers evolving down to very low cutoffs and large numbers of emitted gluons. Formalism and understanding have been refined enormously, and coherence phenomena offer a bridge between shower and string phenomenology. Nevertheless, many implementation details related to parton showers are open and will most likely not be resolved until higher-energy machines become available.

String fragmentation models with normal mesons and baryons as primary particles (as opposed to clusters) are definitely preferred by the data, and at the same time provide a powerful framework for extensions such as the "UCLA-model" for particle composition, such as the approaches to give a consistent description of the entire evolution without the artificial break in a perturbative and a nonperturbative phase, or such as the implementation of effects of quantum statistics.

One may ask why the (Lund) string model is so successful. Of course, one answer is that it really is the "best" phenomenology. Another, that it is the model with the largest number of free parameters. A third, that the Lund group has invested significantly more manpower into the development than any other model maker has. The truth is probably that there is a little of each.

Baryons are emerging as a powerful tool to study the hadronization process, and are likely to provide deeper insight into the fragmentation process as soon as sufficiently large data samples are available; first results look very promising.

While longitudinal and transverse fragmentation functions of gluon jets reveal no surprises, their particle composition is still not very well understood and offers an interesting challenge to both phenomenologists and experimenters.

ACKNOWLEDGEMENT

This work was supported by the U.S. Department of Energy under Contract No. DE-AC03-76SF00098. The author acknowledges receipt of an A.P. Sloan Fellowship.

REFERENCES

1 K. Konishi, A. Ukawa and G. Veneziano, Phys. Lett. 78B (1978) 243; 80B (1979) 259; P. Cvitanovic, P. Hoyer, K. Zalewski, Nucl. Phys. B176 (1980) 429

2 G. Altarelli and G. Parisi, Nucl. Phys. B126 (1977) 298

3 A.H. Muller, Phys. Lett. 104B (1981) 161; B.I.Ermolaev and V.S. Fadin, JETP Lett. 33 (1981) 269; A. Basetto, C. Ciafaloni and G. Marchesini, Phys. Rep. 100 (1983) 201; G. Marchesini and B.R. Webber: Nucl. Phys. B238 (1984) 1

4 D. Amati and G. Veneziano, Phys. Lett. 83B (1979) 87

5 Using the Lund Monte Carlo Jetset 6.3 with default parameters

6 G. Marchesini, Proc. UCLA Workshop on Standard Model Physics at the SSC, ed. H.U. Bengtsson et al., p 114 (1986)

7 M. Bengtsson and T. Sjöstrand, Nucl. Phys. B289 (1987) 810

8 D. Amati et al., Nucl. Phys. B173 (1980) 429; G. Curci, W. Furmanski and R. Petronzio, Nucl. Phys. B175 (1980) 27

9 B.R. Webber, Nucl. Phys. B238 (1984) 492

10 M. Bengtsson and T. Sjöstrand, Phys. Lett. 185B (1987) 435

11 T.D. Gottschalk, Proc. UCLA Workshop on Standard Model Physics at the SSC, ed. H.U. Bengtsson et al., p. 122 (1986)

12 R. Odorico, Z. Phys. C30 (1986) 257

13 The name "cluster model" for QCD shower models is somewhat of a historical misnomer, since recent versions of string models also produce clusters as primary objects, while on the other hand recent shower models create both ordinary particles and clusters in the preconfinement process.

14 G.C. Fox and S. Wolfram: Nucl. Phys. B168 (1980) 285

15 R.D. Field and S. Wolfram: Nucl. Phys. B213 (1983) 65

[16] T.D. Gottschalk, Nucl. Phys. B239 (1984) 349

[17] The actual number of "free" parameters in a model is sometimes hard to determine, since some of the parameters e.g. in the Lund model have virtually no influence on the simulation; they are included as parameters for the sole reason to demonstrate that the model is insensitive to these quantities.

[18] B. Andersson et al., Phys. Rep. 97 (1983) 31

[19] X. Artru, Phys. Rep. 97 (1987) 1; A. Casher, H. Neuberger and S. Nussinov, Phys. Rev. D20 (1979) 179; D21 (1980) 1966

[20] J. Schwinger, Phys. Rev. 128 (1962) 2425

[21] T. Sjöstrand, Computer Phys. Comm. 39 (1986) 347; 28 (1983) 229; 27 (1982) 243

[22] T.D. Gottschalk and D.A. Morris, Nucl. Phys. B288 (1987) 729

[23] T.D. Gottschalk, Nucl. Phys. B239 (1984) 325

[24] W. Bartel et al. (JADE), Z. Phys. C33 (1986) 23

[25] W. Braunschweig et al. (TASSO), paper submitted to this conf.

[26] M. Arneodo et al. (EMC), Phys. Lett. 149B (1984) 415

[27] M. Arneodo et al. (EMC), CERN-EP/87-112 (1987), subm. to Z. Phys. C

[28] P.M. Stevenson, Nucl. Phys. B156 (1979) 43; R.D. Peccei, R. Rückl, Nucl. Phys. B182 (1981) 21

[29] B. Andersson, G. Gustafson and T. Sjöstrand, Z. Phys. C12 (1982) 49

[30] M. Bengtsson, T. Sjöstrand, G. Ingelman, DESY 87/097 (1987)

[31] T. Takahashi, Proc. XXII Rencontre de Moriond, 1987

[32] Ya. I. Azimov et al., Phys. Lett. 165B (1985) 147

[33] W. Bartel et al. (JADE), Phys. Lett. 101B (1981) 129; 134B (1984) 275; 157B (1985) 340; H. Aihara et al. (TPC), Z. Phys. C28 (1985) 31; M. Althoff et al. (TASSO), Z. Phys. C29 (1985) 29

[34] H. Aihara et al. (TPC), Phys. Rev. Lett. 57 (1986) 945; P. Sheldon et al. (MARK II), Phys. Rev. Lett. 57 (1986) 1398; W. Bartel et al. (JADE), paper submitted to this conf.

[35] A. Petersen et al. (MARK II), SLAC-PUB-4290 (1987)

[36] D. Bender et al. (HRS), Phys. Rev. D31 (1985) 1

[37] Note that correlations between data points in related distributions (such as thrust and sphericity) are taken into account in the calculation of χ^2; one should therefore not attempt to interprete the resulting χ^2 in a strictly statistical sense.

[38] C.D. Buchanan and S.B. Chun, UCLA-87-005 (1987), subm. to Phys. Rev. Lett.

[39] For reviews and further refs. see A. Wroblewski, Acta Phys. Pol. B16 (1985) 379; P.K. Malhotra and R. Orawa, Z. Phys. C17 (1983) 85; W. Hofmann, LBL-23921 (1987)

[40] M. Arneodo et al. (EMC), Z. Phys. C34 (1987) 283; G.T. Jones et al., Z. Phys. C27 (1985) 43; I. Cohen et al., Phys. Rev. Lett. 40 (1978) 1614; W. Bartel et al. (JADE), Z. Phys. C20 (1983) 187; M. Derrick et al. (HRS), Phys. Lett. 158B (1985) 519; M. Althoff et al. (TASSO), Z. Phys. C27 (1985) 27

[41] H. Aihara et al. (TPC), submitted to this conf.

[42] H. Aihara et al. (TPC), Phys. Rev. Lett. 52 (1984) 577

[43] M. Althoff et al. (TASSO), Z. Phys. C17 (1983) 5; and paper subm. to 1985 Int. Symp. on Lepton and Photon Int., Kyoto (1985)

[44] W. Braunschweig et al. (TASSO), Z. Phys. C33 (1986) 13

[45] S. Brodsky and G. Farrar, Phys. Rev. Lett. 31 (1973) 1153; V.A. Matveev et al, Nuovo Cimento Lett. 1 (1973) 719; S. Brodsky and J. Gunion, Phys. Rev. D17 (1978) 848

[46] S. Abachi et al. (HRS), ANL-HEP-CP-87-60 (1987), submitted to this conference

[47] W. Bartel et al. (JADE), Z. Phys. C28 (1985) 343

[48] A. Drescher, Ph. D. Thesis, Dortmund (1987)

[49] Also, the MARK II experiment finds η rates consistent with the JADE data and with the Lund model. J. Dorfan, priv. comm.

[50] M. Derrick et al. (HRS), Phys. Lett. 158B (1985) 519; S. Abachi et al. (HRS), Phys. Rev. Lett. 57 (1986) 1990; ANL-HEP-CP-87-71 (1987), submitted to this conference

[51] D.B. MacFarlane, Proc. XXIII Int. Conf. on High Energy Physics, Berkeley (1986), p. 664; C. Bebek et al. (CLEO), paper submitted to this conf.

[52] Recent attempts to fit many parameters and data sets simultaneously improve the situation somewhat; still, however, it is technically impossible to allow all potentially relevant parameters to vary - the fit would not converge in a finite time. Worse, even if the fit succeeds, it may improve our knowledge of some "engineering constants", but it usually will not further our intuitive understanding of the underlying physics.

[53] H. Aihara et al. (TPC), Phys. Rev. Lett. 55 (1985) 1047

[54] H. Aihara et al. (TPC), Phys. Rev. Lett. 57 (1986) 3140

[55] In order to eliminate backgrounds from secondary protons, the study uses only antiprotons.

[56] Using the Feynman-Field option provided in the Lund Monte Carlo.

[57] B. Andersson, G. Gustafson and T. Sjöstrand, Nucl. Phys. B197 (1982) 45; T. Meyer, Z. Phys. C12 (1982) 77; E.M. Iglenfritz, J. Kripfganz and A. Schiller, Acta Phys. Pol. B9 (1978)

881; A. Bartl, H. Fraas and W. Majoretto, Phys. Rev. D26 (1982) 1061; for more refs. see B.O. Shytt, TRITA-FFY-87-04 (1987)

[58] A. Casher, H. Neuberger and S. Nussinov, Phys. Rev. D20 (1979) 179; B. Andersson, G. Gustafson and T. Sjöstrand, Physica Scripta 32 (1985) 574

[59] R.D. Field, R.P. Feynman, Nucl. Phys. B136 (1978) 1

[60] B. Andersson, G. Gustafson abd B. Söderberg, Z. Phys. C20 (1983) 317

[61] M.G. Bowler, Z. Phys. C22 (1984) 155; C11 (1981) 169

[62] S. Klein et al. (MARK II), Phys. Rev. Lett. 58 (1987) 664

[63] S. Abachi et al. (HRS), ANL-HEP-PR-87-26 (1987), subm. to this conference

[64] A. Albrecht et al. (ARGUS), Phys. Lett. 183B (1987) 419 and papers submitted to this conf.

[65] S. Behrends et al. (CLEO), Phys. Rev. D31 (1985) 2161; M. Althoff et al. (TASSO), Physl.Lett. 130 (1983) 340

[66] M. Althoff et al. (TASSO), Z. Phys. C26 (1984) 181

[67] H. Aihara et al., Phys. Rev. Lett. 54 (1985) 274

[68] M. Arneodo et al., Z. Phys. C34 (1987) 283

[69] P. Baringer et al. (HRS), Phys. Rev. Lett. 56 (1986) 1346

[70] S. Brodsky and J.F. Gunion, Phys. Rev. Lett. 37 (1976) 402

[71] A. Petersen et al. (MARK II), Phys. Rev. Lett. 55 (1985) 1954

[72] G. Arnison et al. (UA1), Nucl. Phys. B276 (1986) 253

[73] H.J. Behrend et al. (CELLO), paper submitted to this conf.

[74] R.D. Field, Phys. Lett. 135B (1984) 203

[75] C. Petersen and T.F. Walsh, Phys. Lett. 91B (1980) 455

[76] W. Hofmann, Proc. XVI Int. Symp. on Multiparticle Dynamics, Kiryat Anavim (1985), p. 635

[77] X. Artru, Z. Phys. C26 (1984) 83

[78] For reviews and further refs, see G. Goldhaber, Proc. LESIP I Workshop, Bad Honnef (1984); G. Goldhaber and I. Juricic, Proc. LESIP II Workshop, Santa Fe (1986); W. Hofmann, Proc. Workshop on Electronuclear Physics, SLAC (1987), p. 174

[79] B. Andersson and W. Hofmann, Phys. Lett. 169B (1986) 364

[80] M.G. Bowler and X. Artru, Oxford preprint 79/86 1986)

[81] See also M.G. Bowler, Z. Phys. C29 (1985) 617; Phys. Lett. 180B (1986) 299; 185B (1987) 205

[82] B. Andersson, G. Gustafson and B. Söderberg, Nucl. Phys. B264 (1986) 29

LAWRENCE BERKELEY LABORATORY
TECHNICAL INFORMATION DEPARTMENT
UNIVERSITY OF CALIFORNIA
BERKELEY, CALIFORNIA 94720